Journal for ImmunoTherapy of Cancer

PD-L1 CAR effector cells induce self-amplifying cytotoxic effects against target cells

Malgorzata Bajor,[1,2] Agnieszka Graczyk-Jarzynka,[2,3] Katsiaryna Marhelava,[1,4,5] Anna Burdzinska,[6] Angelika Muchowicz,[3] Agnieszka Goral,[3] Andriy Zhylko,[3,7] Karolina Soroczynska,[3] Kuba Retecki,[3] Marta Krawczyk,[2,3,5,8] Marta Klopotowska,[1,2] Zofia Pilch,[3] Leszek Paczek,[6,9] Karl-Johan Malmberg,[10] Sébastien Wälchli,[11] Magdalena Winiarska ,[3] Radoslaw Zagozdzon [1,5,9,12]

To cite: Bajor M, Graczyk-Jarzynka A, Marhelava K, *et al*. PD-L1 CAR effector cells induce self-amplifying cytotoxic effects against target cells. *Journal for ImmunoTherapy of Cancer* 2022;**10**:e002500. doi:10.1136/jitc-2021-002500

► Additional supplemental material is published online only. To view, please visit the journal online (http://dx.doi.org/10.1136/jitc-2021-002500).

MB, AG-J and KM contributed equally.

Accepted 19 December 2021

For numbered affiliations see end of article.

Correspondence to
Dr Magdalena Winiarska; mwiniarska@wum.edu.pl

Dr Radoslaw Zagozdzon; radoslaw.zagozdzon@wum.edu.pl

ABSTRACT

Background Immune checkpoint inhibitors and chimeric antigen receptor (CAR)-based therapies have transformed cancer treatment. Recently, combining these approaches into a strategy of PD-L1-targeted CAR has been proposed to target PD-L1^{high} tumors. Our study provides new information on the efficacy of such an approach against PD-L1^{low} targets.

Methods New atezolizumab-based PD-L1-targeted CAR was generated and introduced into T, NK, or NK-92 cells. Breast cancer MDA-MB-231 and MCF-7 cell lines or non-malignant cells (HEK293T, HMEC, MCF-10A, or BM-MSC) were used as targets to assess the reactivity or cytotoxic activity of the PD-L1–CAR-bearing immune effector cells. Stimulation with IFNγ or with supernatants from activated CAR T cells were used to induce upregulation of PD-L1 molecule expression on the target cells. HER2–CAR T cells were used for combination with PD-L1–CAR T cells against MCF-7 cells.

Results PD-L1–CAR effector cells responded vigorously with degranulation and cytokine production to PD-L1^{high} MDA-MB-231 cells, but not to PD-L1^{low} MCF-7 cells. However, in long-term killing assays, both MDA-MB-231 and MCF-7 cells were eliminated by the PD-L1–CAR cells, although with a delay in the case of PD-L1^{low} MCF-7 cells. Notably, the coculture of MCF-7 cells with activated PD-L1–CAR cells led to bystander induction of PD-L1 expression on MCF-7 cells and to the unique self-amplifying effect of the PD-L1–CAR cells. Accordingly, PD-L1–CAR T cells were active not only against MDA-MD-231 and MCF-7-PD-L1 but also against MCF-7-pLVX cells in tumor xenograft models. Importantly, we have also observed potent cytotoxic effects of PD-L1–CAR cells against non-malignant MCF-10A, HMEC, and BM-MSC cells, but not against HEK293T cells that initially did not express PD-L1 and were unresponsive to the stimulation . Finally, we have observed that HER-2–CAR T cells stimulate PD-L1 expression on MCF-7 cells and therefore accelerate the functionality of PD-L1–CAR T cells when used in combination.

Conclusions In summary, our studies show that CAR-effector cells trigger the expression of PD-L1 on target cells, which in case of PD-L1–CAR results in the unique self-amplification phenomenon. This self-amplifying effect could be responsible for the enhanced cytotoxicity of PD-L1–CAR T cells against both malignant and non-malignant cells and implies extensive caution in introducing PD-L1–CAR strategy into clinical studies.

INTRODUCTION

Chimeric antigen receptor (CAR)-based strategies are one of the major breakthroughs in modern anticancer therapies. A crucial issue in designing CAR-based therapy is selecting a specific and safe target to ensure a proper balance between strength and precision. In the early studies, CD19, a surface marker of B cells, was identified as one of the most promising molecules for such interventions, as it is uniformly expressed on most B-cell-derived malignancies. To date, five CAR-based strategies have been approved by the U.S. Food and Drug Administration (FDA) for hemato–oncological applications. However, while CAR-based approaches have been applied in hematological malignancies with considerable success, their effectiveness in solid tumors treatment is modest at best. One of the reasons for this phenomenon is the immunosuppressive environment at the tumor site, which can be mediated by the expression of immune checkpoint molecules, such as programmed death-ligand 1 (PD-L1, CD274) acting on its cognate receptor PD-1 (CD279) on the immune effector cells.[1] PD-L1 can be present either directly on cancer cells or on other cells in the tumor microenvironment (TME),[2 3] making TME a formidable opponent of CAR T-based therapies. This has brought an idea of combining anti-PD-L1 approaches with CAR-based treatment.[3 4] Thus, the anti-PD-1/PD-L1 targeting has indeed been attempted by numerous research groups in order to increase the potency of CAR T-based approaches (reviewed by Tang *et al* and Yoon *et al*).[4 5] An extension

of this idea was the generation of PD-L1-targeting CAR constructs. Accordingly, the PD-1- or atezolizumab-based CARs were very recently reported to act against cancer cells expressing high amounts of PD-L1. Moreover, in addition to direct killing of the PD-L1-expressing cancer cells, the PD-L1–CAR-bearing immune effector cells have shown the ability to reshape the TME,[6] by eliminating the tumor-infiltrating macrophages and neutrophilic and monocytic myeloid cells endogenously expressing high levels of PD-L1.[7] Additionally, multiple healthy cells were demonstrated to express detectable levels of PD-L1 in steady state or on induction.[8]

In the current work, we have observed that PD-L1–CAR cells stimulate PD-L1 expression on target tumor PD-L1^{low} cells. We have also investigated how non-malignant cells, with initially high or low/null expression of PD-L1, respond to the PD-L1–CAR-bearing effectors. Consequently, we present new data on the responsiveness in vitro and in vivo of both malignant and non-malignant PD-L1^{low} target cells to PD-L1–CAR effector cells due to the unique self-amplifying ability of this therapeutic approach. Our results help to understand the mechanisms of potential non-selectivity of the PD-L1–CAR regarding the on-target, off-tumor effect. Moreover, we demonstrate that the PD-L1 induction phenomenon after treatment with CAR T cells is also observed for human epidermal growth factor receptor 2(HER-2)–CAR. In this setting, PD-L1–CAR could be further explored to potentiate the antitumor activity of CAR-based approaches in the therapy of solid tumors. Hereby, we propose a sequential approach involving the prior application of HER-2–CAR as an exemplary tumor-specific CAR, promoting the functionality of PD-L1–CAR when used in combination.

MATERIALS AND METHODS

All materials and methods are available in the online supplemental file.

RESULTS

PD-L1 as a target for CAR-based therapy

Since PD-L1 within tumor mass can be observed on both tumor cells and TME cells, we performed screening experiments to determine the PD-L1 expression in various cell types. In the first step, we identified the PD-L1-positive tumor cells in a set of 18 cell lines derived from various cancers by western blotting. As shown in figure 1A and online supplemental figure 1A, detectable levels of PD-L1 protein expression were observed in a proportion of cell lines derived from breast cancer, particularly of the triple-negative phenotype (MDA-MB-231—PD-L1^{high}, HCC-1806—PD-L1$^{moderate/low}$), ovarian cancer (OvCa3, MDAH), Hodgkin's lymphoma (SUO-HD1, HDLM-2), or malignant melanoma (M257). In a further study, we decided to focus on breast cancer models, as the expression of PD-L1 protein in this cancer significantly correlates with survival outcome in patients with mammary malignancies.[9 10] Notably, our results of the variable expression of PD-L1 in breast cancer cell lines are in accordance with previous observations in primary mammary malignancies.[11] Therefore, our data support the notion that a proportion of breast cancers, especially of triple-negative phenotype, could potentially be directly targeted by PD-L1–CAR. As the surface expression of the target molecule is crucial for the CAR efficacy, we have validated PD-L1 expression by flow cytometry using two anti-PD-L1 monoclonal antibodies: MIH-1 clone (figure 1B for MCF-7 and MDA-MB-231 and online supplemental figure 1B for HCC1806) and 29E.2A3 clone (online supplemental figure 1C). Consequently, MCF-7 cells (PD-L1$^{low/null}$) and MDA-MB-231 cells (PD-L1^{high}) were used as predominant models in our study.

Additionally, as a significant percentage of mammary tumors exhibit PD-L1 expression also in their stroma,[12] in the next step, we evaluated the PD-L1 protein expression in macrophages, which are known as key contributors of tumor stroma formation.[13 14] We have studied the PD-L1 expression using immunofluorescent microscopy in the M0, interferon γ (IFNγ)-stimulated M0, and M2 phenotypes; additionally, CD206 as a characteristic marker for the M2 phenotype was used. As shown in figure 1C, while in the M0 phenotype, the expression of PD-L1 protein was undetectable, the IFNγ-stimulated macrophages or those differentiated into M2 phenotype exhibited high intensity of PD-L1 staining. These findings indicate that the macrophages attributed to the intratumoral immunosuppressive microenvironment can constitute a potential target for the PD-L1–CAR strategy.

Generation and expression of PD-L1–CAR in immune effector cells

We generated a new atezolizumab-based single-chain variable fragment (scFv) and combined it with a standard second-generation CAR backbone comprised of IgG4 hinge region, CD28 transmembrane and signaling portions, and the CD3ζ signaling domain (figure 2A). For the stable long-term exogenous expression, lentiviral transduction was used, and CAR expression was evaluated by the anti-Fc staining (figure 2B and online supplemental figure 2A). We also introduced PD-L1–CAR into NK cells by electroporation (online supplemental figure 2B) or into NK-92 cells by lentiviral transduction (figure 2C). NK-92 cells were further enriched in the PD-L1–CAR-positive population, up to approximately 90% (online supplemental figure 2C) by sorting. In subsequent experiments, we used both T cells or NK cells based models of CAR-engineered effector cells to determine the antitumor activity of the PD-L1 CAR-based approaches.

Importantly, we observed that the stimulation of T cells with CD3/CD28 beads prior to modification led to the PD-L1 upregulation already after 24 hours, which remained high until day 4 and decreased back to initial expression ranges by day 6 (figure 2D), posing the potential risk of the fratricidal killing. To address this issue, the CD19–CAR T (online supplemental figure 3A) or

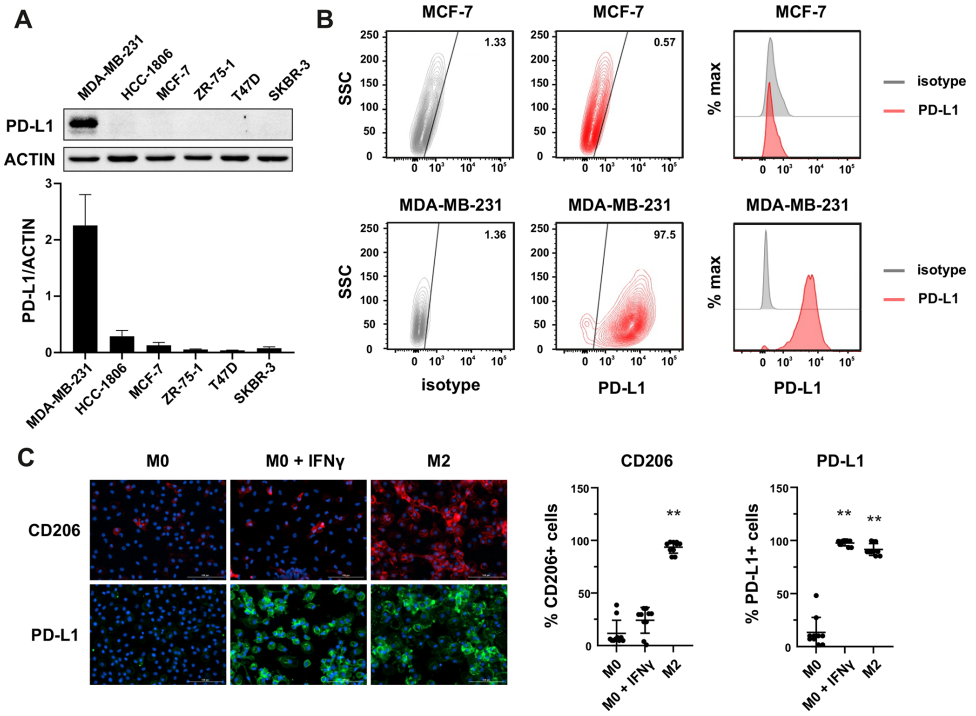

Figure 1 Expression of PD-L1 in breast cancer cell lines and macrophages. (A) The representative western blot analysis of PD-L1 expression in triple-negative (MDA-MB-231, HCC-1806), ER-positive (MCF-7, ZR-75-1, T47D), and HER-2-positive (SKBR-3) breast cancer cell lines (upper panel). β-actin was used as a loading control. The experiment was repeated three times. Bands were quantified by densitometry; the signal for PD-L1 band was normalized to the corresponding actin band (lower panel). (B) Representative density plots and histogram overlays illustrating PD-L1 expression (red) against a background from isotype control (gray) for MCF-7 (upper panel) and MDA-MB-231 (lower panel) breast cancer cell lines using flow cytometry. The staining was performed using an anti-PD-L1 antibody (cat. no. 12-5983-42, eBioscience, clone MIH1, dilution 1:100). Numbers on the density plots indicate the percentage of PD-L1-positive cells. The experiment was repeated at least three times. (C) PD-L1 expression in macrophage subpopulations (M0, M0+IFNγ, M2) detected by immunocytohistochemistry assay using Cytation 1 Cell Imaging Multi-Mode Reader (BioTek, Agilent). PD-L1 positively stained cells were detected using an anti-PD-L1 antibody (clone MIH1, cat. no. 14-5983-82, eBioscience, dilution 1:100) and are marked in green; red shows CD206-positive cells (cat. no. AF2534, R&D Systems, dilution 1:100). The signal was developed using AF488-conjugated or AF647-conjugated secondary antibody, respectively, and nuclei were counterstained with DAPI (blue). Bar graphs represent the quantitative analysis of either CD206 or PD-L1 expression in different macrophage subpopulations as a percentage of all cells. Data aggregated from three experiments performed in duplicates with two to four donors in each experiment (n=10). Bars represent the mean value±SD. The normality was checked using the Shapiro-Wilk test. The p values derived from Wilcoxon test (comparing to control): **p<0.01. PD-L1, programmed death-ligand 1, HER2, human epidermal growth factor receptor 2, IFNγ, interferon γ, DAPI, blue-fluorescent DNA stain (4′,6-diamidino-2-phenylindole).

PD-L1–CAR T cells, 48 hours after lentiviral transduction with respective CAR-encoding vectors, were stimulated with the anti-CD3/anti-CD28-coated beads, and the dynamics of PD-L1 surface expression was assessed by flow cytometry. As shown in online supplemental figure 3B, the dynamics of PD-L1 expression in CD19–CAR T cells resembled the ones in primary T lymphocytes (figure 2D). However, no apparent induction of PD-L1 expression was detected in PD-L1–CAR T cells. In order to get a closer insight into this subject, we further documented the general capability of fratricidal killing by PD-L1–CAR T cells in coculture experiments with genetically unmodified activated T cells (online supplemental figure 3C). Our results clearly indicate that bead-stimulated unmodified T cells are indeed eliminated by PD-L1–CAR-bearing T cells and this effect is alleviated by atezolizumab. Furthermore, we performed western blotting to assess the general content of PD-L1 protein in CAR-bearing cells (online supplemental figure 3D) and the results were closely corresponding to the flow cytometry-based observations. Altogether, our data indicated that by expressing the PD-L1–CAR in T cells, we have here generated a unique population of T cells with suppressed expression of PD-L1 protein. Surprisingly, when we studied PD-L1 mRNA expression in these cells by qPCR (online supplemental figure 3E), the expression pattern was closely resembling the ones in unmodified and CD19–CAR T cells, that is, PD-L1–CAR T cells were clearly capable of inducing PD-L1 mRNA expression following stimulation. This suggests that the mechanism of PD-L1 protein suppression is post-transcriptional. We find this observation highly interesting from the biological point of view and worth exploring in future investigations. Moreover, we have carried out phenotyping of CD19- versus PD-L1-CAR-T cells on days 4 and 10 following transduction (online supplemental figure 3F).

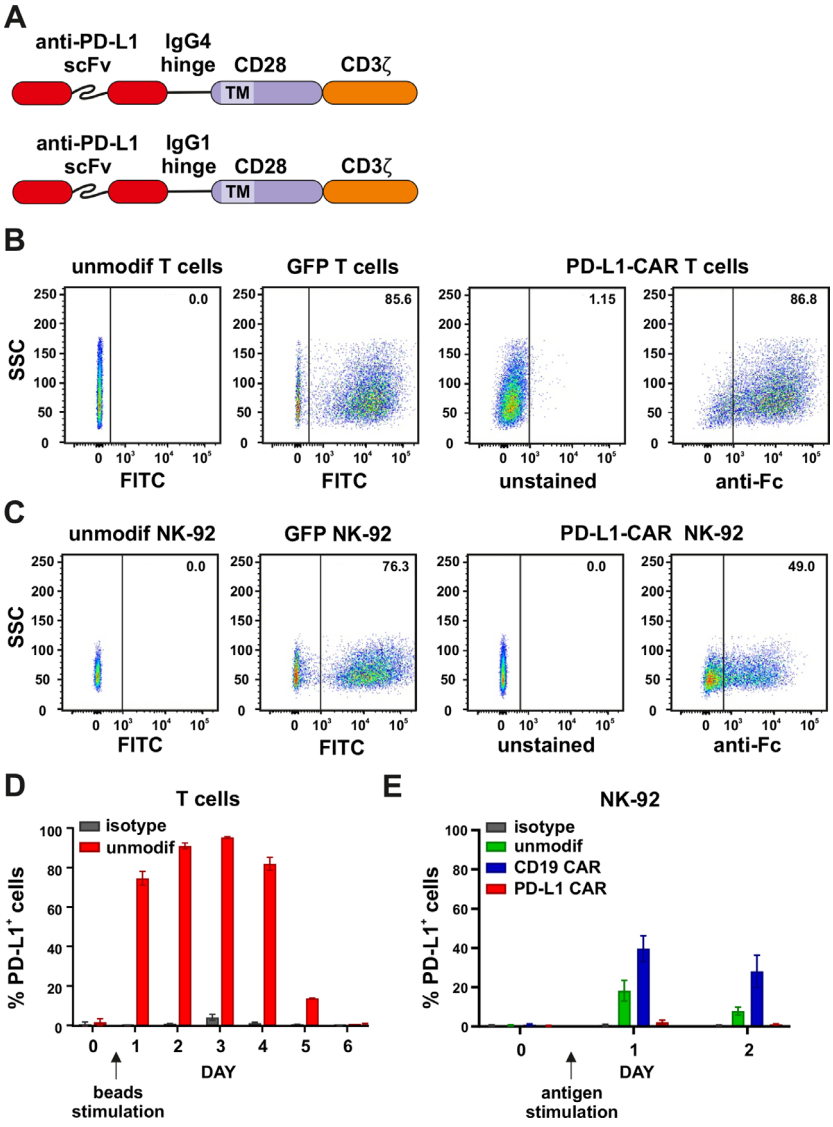

Figure 2 Generation and expression of PD-L1–CAR in immune effector cells. (A) The scheme depicting the modular structure of PD-L1–CARs used in the study (in detail described in the Materials and methods section). (B) Flow cytometry analysis of GFP (left panels) or PD-L1–CAR (right panels) expression in T cells after lentiviral transduction. GFP expression was detected in FITC channel and PD-L1–CAR expression was detected using anti-human IgG, Fcγ fragment specific antibody (cat. no. 109-606-098, Jackson ImmunoResearch). Numbers on the density plots indicate the percentage of PD-L1–CAR-positive cells. The experiments were repeated at least three times. (C) Flow cytometry analysis of GFP (left panels) or PD-L1–CAR (right panels) expression in NK-92 cells after lentiviral transduction was performed as described in (B). (D) PD-L1 expression on primary T cells. Bar graphs represent PD-L1 expression on unmodified effector cells T cells. T cells were cultivated in the presence of 100 U/mL of IL-2 alone (day 0) or together with human T-activator CD3/CD28 beads (days 1–6). Day 1 represents the first day after the stimulation of T cells with human T-activator CD3/CD28 beads. PD-L1 staining was performed on consecutive days using an anti-PD-L1 antibody (clone 29E.2A3, dilution 1:100). The experiment was repeated in duplicates two times. (E) PD-L1 expression on NK-92 cell line. Flow cytometry analysis of PD-L1 expression in NK-92, CD19–CAR NK-92, and PD-L1–CAR NK-92 cells following the stimulation with target Raji PD-L1 cells. The effector cells were coincubated with targets in a 1:1 E:T ratio. The PD-L1 expression on NK-92, CD19–CAR and PD-L1–CAR NK-92 cells was assessed 24 and 48 hours after the stimulation using an anti-PD-L1 antibody (clone MIH1, cat. no. 14-5983-82, eBioscience, diluted 1:100). Bar graphs represent the percentage of PD-L1-positive cells. The experiment was repeated three times. CAR, chimeric antigen receptor, PD-L1, programmed death-ligand 1, GFP, green fluorescent protein, FITC, fluorescein isothiocynate, scFV, single-chain variable fragment

While we did detect differences in PD-L1 expression, in concordance with other results in our study, we did not see significant differences in other activation/exhaustion markers, apart from a change in PD-1 expression on day 4.

To compare, we also evaluated the NK-92 cell line (figure 2E) for the capability of inducing PD-L1 protein expression after target-specific stimulation. Again, as presented in figure 2E, we observed that unmodified (ie, naturally cytotoxic) or CD19–CAR-bearing NK-92

cells have responded to the target stimulus (ie, Raji–PD-L1 cells) with an increase of PD-L1 expression, while the PD-L1–CAR-bearing NK-92 cells retained the PD-L1 membrane presence at undetectable levels.

The activity of PD-L1–CAR effector cells against tumor cells

To investigate the efficacy of a newly generated PD-L1–CAR against breast cancer cell lines, PD-L1–CAR T cells or NK cells were incubated with target MDA-MB-231 (PD-L1^{high}) or MCF-7 (PD-L1$^{low/null}$) cells. Degranulation of CAR T cells assessed by CD107a staining and tumor necrosis factor α (TNFα) or IFNγ production was compared with the effector cells transduced with green fluorescent protein(GFP)-encoding control vector. As expected, only incubation with MDA-MB-231 induced both potent degranulation and cytokines' production by PD-L1–CAR T cells (figure 3A), PD-L1–CAR–NK-92 cells (online supplemental figure 4A), or PD-L1–CAR–NK cells within 4 hours (online supplemental figure 4B). To verify the specificity of the new PD-L1–CAR, we generated the PD-L1-knockout (KO) derivatives of MDA-MB-231 cell line (MDA-MB-231-sgPD-L1; online supplemental figure 4C,D) and also the PD-L1-overexpressing derivative of MCF-7 cell line (MCF-7-PD-L1; online supplemental figure 4E,F). When incubated with PD-L1–CAR T cells, MDA-MB-231-sgPD-L1 cells significantly decreased the effector cells' degranulation and cytokines' production, and the opposite effect was observed with MCF-7-PD-L1 cells (figure 3B for PD-L1–CAR T cells and online supplemental figure 4G for PD-L1–CAR–NK-92 cells).

To directly assess the cytotoxicity of PD-L1–CAR T cells, we performed real-time cell assays (RTCA) with MDA-MB-231 or MCF-7 cells. Surprisingly, a potent, E:T ratio-dependent, cytotoxic effect was seen against both types of cells, although it was delayed in the case of MCF-7 cells (figure 3C vs D, right panels, for MDA-MB-231 and MCF-7 cells, respectively). To confirm, that the delayed effectiveness of PD-L1–CAR T cells against PD-L1^{low} target cells is not unique for MCF-7, we have used another PD-L1^{low} cell line, namely T47D cells. As presented in online supplemental figure 4H, T47D cells were also successfully eliminated by PD-L1–CAR T cells, again with the cytotoxicity onset delayed by approximately 4–6 hours. Because of these surprizing observations, we further verified the specificity of PD-L1–CAR and used atezolizumab in order to block the binding of PD-L1–CAR T to its target competitively. Incubation with atezolizumab abrogated the cytotoxic effects of PD-L1–CAR T cells against the MDA-MB-231 (figure 4A, left panel) and also against MCF-7 cells (figure 4A, right panel). Moreover, in agreement with our previous results, the cytotoxicity of PD-L1–CAR T cells against the MDA-MB-231-sgPD-L1 cells was strongly diminished in the RTCA assay as compared with the MDA-MB-231-sgNTC controls (figure 4B), further confirming the specificity of PD-L1–CAR.

The introduction of PD-L1 into the MCF-7 line led to a rapid eradication by PD-L1 CAR cells (figure 4C, middle panel). Corroborating the initial observation in the parental MCF-7 (figure 3D), also the MCF-7-pLVX controls were eradicated although again with a slight delay (figure 4C, left). Indeed, the latency in the appearance of the CAR-mediated killing in MCF-7- PD-L1$^{low/null}$ types of cells suggests that PD-L1 molecule may become upregulated on the MCF-7-pLVX cells with time during the coincubation with CAR-bearing cells.

To establish whether the observations of PD-L1–CAR effectiveness are reflected in the in vivo settings, we have carried out investigations in the MDA-MB-231-derived or MCF-7-derived human-to-mouse tumor xenograft models (figure 4D,E, respectively). First, we have observed that PD-L1–CAR T cells, but not the control treatment (ie, phosphate-buffered saline (PBS), unmodified T cells, and CD19–CAR T cells), induced significant retardation of MDA-MB-231 tumor growth (figure 4D, left-hand panel and online supplemental figure 4I) and prolonged mouse survival (as assessed by reaching the predefined tumor volume; figure 4D, right-hand panel). Importantly, we have also observed induction by PD-L1–CAR T cells of retardation in tumor growth in the models of both MCF-7-pLVX (figure 4E, left-hand panel and online supplemental figure 4J, left-hand panel) and MCF-7-PD-L1 xenografts (figure 4E, right-hand panel and online supplemental figure 4J, right-hand panel), which confirms that PD-L1–CAR can be effective against initially PD-L1 $^{low/null}$ cells in a growing in a living organism.

Altogether, the results described in the current subsection prompted us to elucidate further the mechanisms and dynamics of PD-L1 upregulation on target cells following their interaction with CAR-modified effector cells.

Induction of PD-L1 expression on the target cells

First, we addressed the question whether PD-L1 expression could be increased by antigen-activated CAR T cells in a self-amplifying mechanism. To answer this, we transferred the conditioned supernatants from the coincubation cultures of PD-L1–CAR T or PD-L1-NK-92 cells with the target MDA-MB-231 cells onto the MCF-7 or MDA-MB-231 cells and assessed PD-L1 surface expression by flow cytometry. As depicted in figure 5A, in MCF-7 cells conditioned supernatants from target-activated CAR T/NK-92 cells increased PD-L1 surface expression. Conversely, MDA-MB-231 cells presented uniformly high expression of PD-L1 regardless of the culture conditions, while PD-L1 KO (sgPD-L1) MDA-MB-231 cells were not able to express PD-L1, once incubated in the presence of conditioned supernatants from activated CAR T cells (online supplemental figure 5A). As activated T cells are known to secrete increased quantities of IFNγ, we hypothesized that the effect of CAR-conditioned medium depends on IFNγ production. We thus investigated the effects of IFNγ on surface PD-L1 levels in MDA-MB-231 and MCF-7 cells. IFNγ did not significantly change PD-L1 levels in MDA-MB-231 cells (online supplemental figure 5B, left panel). Simultaneously, MCF-7 cells' surface PD-1 levels increased on IFNγ treatment (online

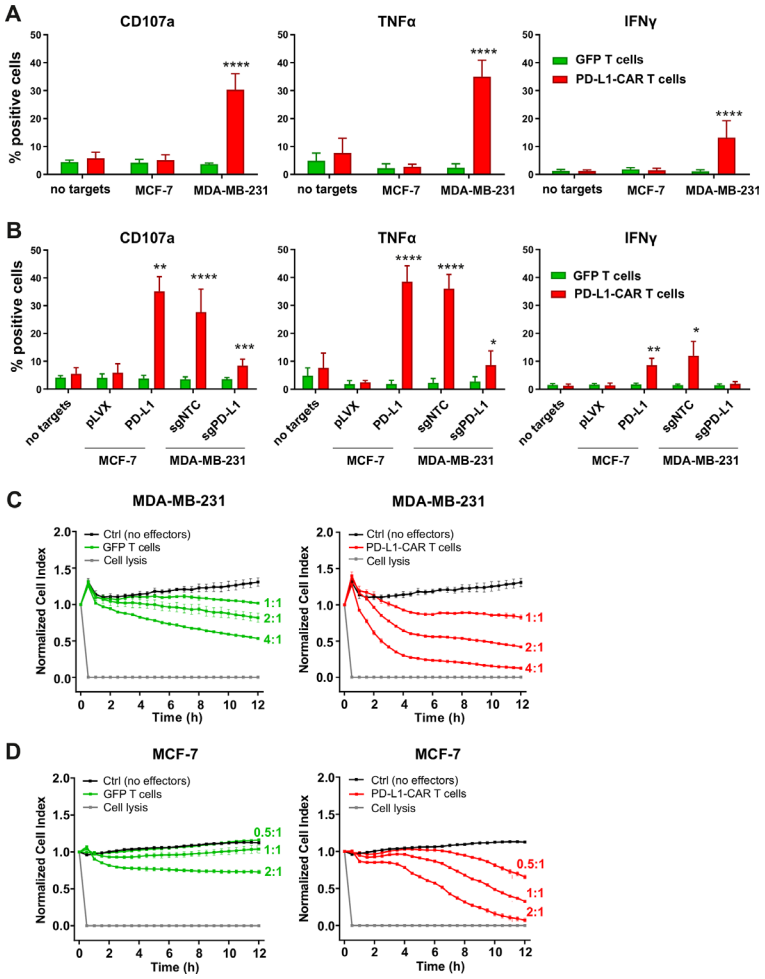

Figure 3 Cytokine production and degranulation by PD-L1–CAR T cells following stimulation with breast cancer cells. (A) Functional and cytokine release assays of PD-L1–CAR T cells targeted against MCF-7 (PD-L1$^{low/-}$) or MDA-MB-231 (PD-L1^{+}) cancer cell lines. Degranulation assay, assessed by CD107a staining (left panel), TNFα release (middle panel), and IFNγ release (right panel) were measured after 4 hours of coincubation of target and effector cells at the E:T ratio of 2:1. The experiment was repeated in duplicates three times. Bars represent the mean value±SD. The normality was checked using the Shapiro-Wilk test. The p values derived from unpaired t-test: ****p<0.0001. (B) Functional and cytokine release assays of PD-L1–CAR T cells targeted against MCF-7 pLVX (PD-L1$^{low/-}$) and MCF-7 PD-L1 and MDA-MB-231 sgNTC (PD-L1^{+}) or MDA-MB-231 sgPD-L1 (PD-L1^{-}) cancer cell lines were assessed by flow cytometry. Degranulation assay, assessed by CD107a staining (left panel), and IFNγ release (right panel) were measured after 4 hours of coincubation of target and effector cells at the E:T ratio of 2:1. The experiment was repeated in duplicate three times (for IFNγ release by MCF-7 for two times). Bars represent the mean value±SD The p values derived from unpaired t-test or Mann-Whitney test depending on data distribution (*p<0.05, **p<0.01, ***p<0.001, ****p<0.0001). (C) The potential of killing tumor cells by control (pSEW-GFP) and PD-L1–CAR T cells was measured by impedance analysis for MDA-MB-231 cells. Cancer cell lines were left to adhere and form a monolayer on the E plates for 24 hours. The next day, PD-L1–CAR T cells or control (pSEW-GFP) T cells were added to the monolayers for 12 hours at the indicated E:T ratios. Representative mean impedance curves from two wells were shown. The experiment was repeated in duplicates two times. (D) The potential of killing tumor cells by control (pSEW-GFP) and PD-L1–CAR T cells was measured by impedance analysis for MCF7 cells. Cancer cell lines were left to adhere and form a monolayer on the E plates for 24 hours. The next day, PD-L1–CAR T cells or control (pSEW-GFP) T cells were added to the monolayers for 12 hours at the indicated E:T ratios. Representative mean impedance curves from two wells were shown. The experiment was repeated in duplicates two times. CAR, chimeric antigen receptor, PD-L1 - programmed death-ligand 1, TNFα - tumor necrosis factor α, IFNγ - interferon γ, GFP - green fluorescent protein, SSC - side scatter

supplemental figure 5B, right panel), however, to a much lesser extent than that observed on incubation with CAR T conditioned medium. Likewise, all three macrophage phenotypes studied (M0, IFNγ-stimulated M0, and M2) responded to the addition of the CAR T/targets conditioned medium with a very potent increase in PD-L1 expression, greatly exceeding those observed for IFNγ only (figure 5B and online supplemental figure 5C). In order to have an insight into the composition of CAR T/NK-92 conditioned media, we performed cytokine arrays, in which we identified a set of cytokines strongly upregulated after antigen-mediated activation of CAR T/NK-92 cells when compared with unmodified T or NK-92 cells, respectively (figure 5C and online supplemental figure

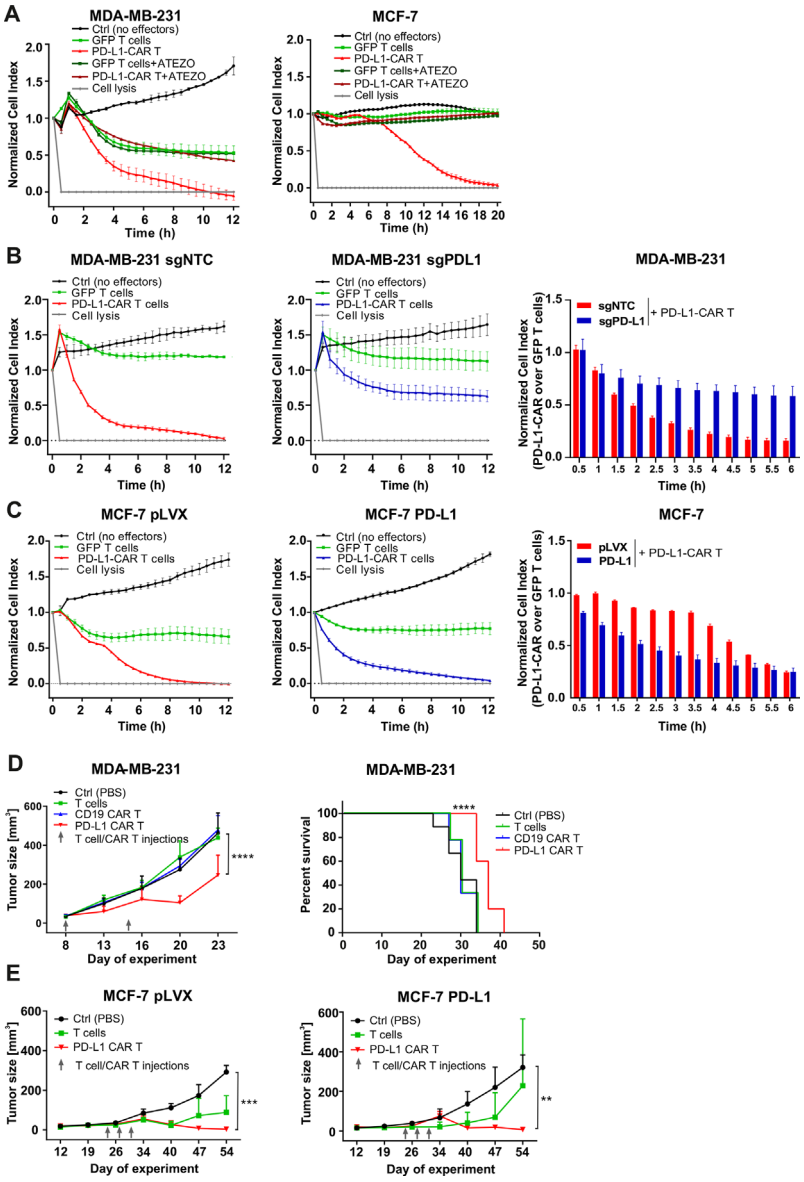

Figure 4 The efficacy of PD-L1–CAR T cells against breast cancer cells with different PD-L1 protein expression. (A) The killing potential of PD-L1–CAR T cells against MDA-MB-231 (left panel) or MCF-7 (right panel) breast cancer cells was measured by impedance analysis. Cancer cell lines were seeded on the E plates and left to adhere and form a monolayer for 24 hours. The next day, PD-L1–CAR T cells or control (pSEW-GFP) T cells were added to the monolayers at the E:T ratio of 2:1 (MDA-MB-231) and 1:1 (MCF-7) in the absence or presence of 0.4 mg/mL atezolizumab. The cultures were monitored for the next 12 hours. Representative mean impedance curves from two wells are shown. The experiment was repeated in duplicates three times. (B) The cytotoxic activity of PD-L1–CAR T cells against MDA-MB-231 sgNTC (left panel) and MDA-MB-231 sgPD-L1 (middle panel) cancer cell lines, at the E:T ratio of 2:1, were measured by impedance analysis. Samples were internally normalized for the cell index value measured before CAR T cells addition (Normalized Cell Index plots). Bar graph represents Normalized Cell Index values of quantification of PD-L1–CAR T-cell killing over GFP T cells control from 0.5 to 6 hours (right panel). Representative average impedance curves from two wells are shown. The experiment was repeated in duplicates two times. (C) Cytotoxic activity of PD-L1–CAR T cells against MCF-7 pLVX (left panel) and MCF-7 PD-L1 (middle panel) cancer cell lines at the E:T ratio of 1:1 were measured by impedance analysis. Samples were internally normalized for the cell index value measured before PD-L1–CAR T cells addition (Normalized Cell Index plots). Bar graph represents Normalized Cell Index values of quantification of PD-L1–CAR T-cell killing over GFP T cells control from 0.5 to 6 hours (right panel). Representative average impedance curves from two wells are shown. The experiment was repeated in duplicates two times. (D) Mean volume of MDA-MB-231 tumors after two rounds (days 8 and 15) of intratumoral administration of PBS (control), unmodified T cells, CD19–CAR or PD-L1–CAR T cells, +SD, two-way ANOVA test, ****p<0.0001, left panel. Corresponding Kaplan-Meier survival plot, analyzed by log-rank survival test, ****p<0.0001, right panel. The graphs present results summarized from two independent experiments, n=9–10. (E) Mean tumor size of MCF-7 pLVX (left panel, n=6–7) and MCF-7 PD-L1 (right panel, n=4–6). Mice were treated with PBS (control), unmodified T cells, or PD-L1–CAR T cells on days 24, 27, and 30, +SD, two-way ANOVA test, **p<0.01, ***p<0.001. CAR, chimeric antigen receptor, PD-L1, programmed death-ligand 1, PBS, phosphate-buffered saline, ANOVA - analysis of variance, GFP - green fluorescent protein.

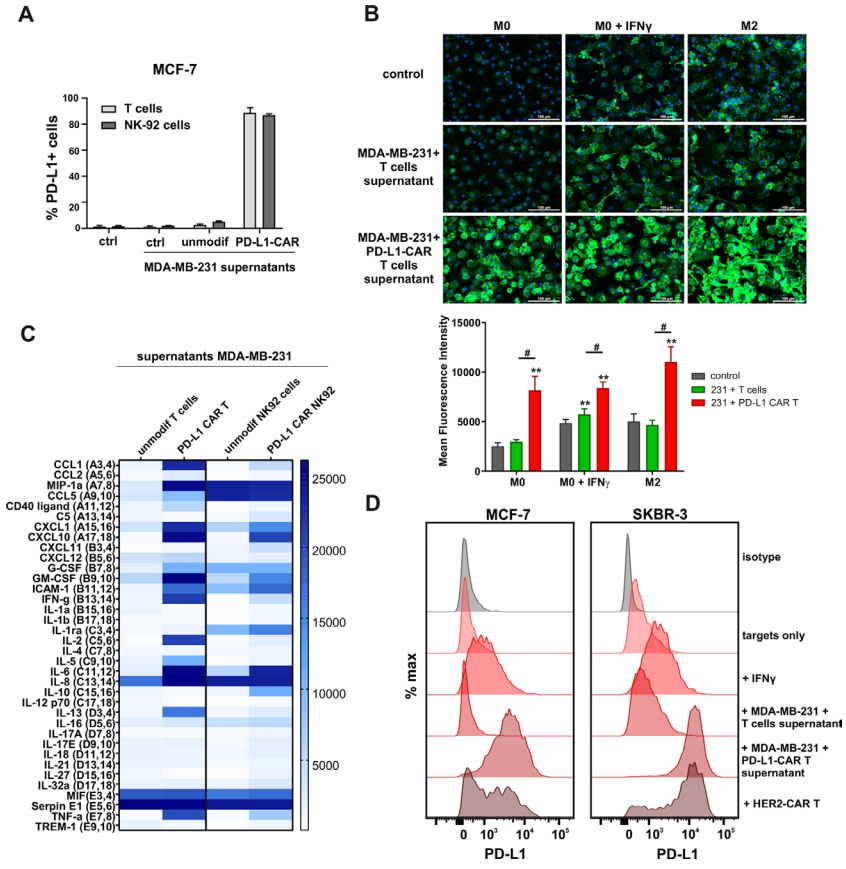

Figure 5 Induction of PD-L1 expression on the target cells. (A) PD-L1 expression induced by supernatant from activated CAR T or CAR–NK-92 cells on cancer cells was assessed by flow cytometry. The control (only medium) and conditioned supernatants from the 24 hours coincubation cultures of control (unmodified) or PD-L1–CAR T/NK-92 cells with the target MDA-MB-231 cells were transferred onto the culture of MCF-7 and incubated for 48 hours. Next, PD-L1 surface presence was assessed using anti-PD-L1 antibody (clone MIH1) by flow cytometry. The experiment was repeated three times. (B) Representative images of different subpopulations of macrophages (M0, M0+IFNγ, M2) stained for PD-L1 assessed by immunocytochemistry assay using Cytation 1 Cell Imaging Multi-Mode Reader (BioTek, Agilent). Macrophages were incubated with 10 ng/mL IFNγ or IL-4 and IL-10 (for M2) for 5 days before staining (every 2-day fresh portion of cytokines was added). The control (only medium) and conditioned supernatants from the 24 hours coincubation cultures of control (unmodified) or PD-L1–CAR T cells with the target MDA-MB-231 cells were transferred onto different subpopulations of macrophages and incubated for 48 hours. Next, PD-L1 surface presence was assessed using anti-PD-L1 antibody (clone MIH1, cat. no. 14-5983-82, eBioscience, diluted 1:100). The signal was developed using AF488-conjugated secondary antibody (green), and nuclei were counterstained with DAPI (blue), scale bar: 100 µm. The background fluorescence was removed, and the low threshold for green fluorescence was set to create a mask of the area covered by macrophages. Bar graphs represent the mean fluorescent intensity of PD-L1 within the thresholded area. Data aggregated from three experiments performed in duplicates with two to four donors in each experiment (n=8–10). Bars represent the mean value±SD. Normality was checked using the Shapiro-Wilk test. The p values derived from Student's t-test or Wilcoxon test (comparing to control), depending on data distribution: **p<0.01. Two-sample Kolmogorov-Smirnov test was used to calculate statistics between T cells and CAR T groups: #p<0.01. (C) The relative levels of human cytokines in supernatants collected from control (unmodified T cells and NK-92 cells) or PD-L1–CAR T cells and NK-92 cells cocultured with MDA-MB-231 breast cancer cells for 24 hours at 1:1 E:T ratio were determined by cytokine array assay. The changes in the expression profile of 36 cytokines are presented on the heat map. The experiment was performed with two donors in duplicates. (D) Representative PD-L1 expression in MCF-7 (left-hand panel) or SKBR-3 (right-hand panel) cells after a 24 hours incubation in the presence of 20 ng/mL IFNγ, supernatants from coculture of unmodified T cells or PD-L1–CAR T cells with MDA-MB-231 and directly with HER2–CAR T cells at 1:1 E:T ratio. PD-L1 surface presence was assessed by flow cytometry using anti-PD-L1 antibody (clone MIH1). The experiment was performed three times in duplicates. CAR, chimeric antigen receptor, PD-L1, programmed death-ligand 1, IFNγ, interferon γ, NK- natural killer, HER2, human epidermal growth factor receptor 2, IL-4, interleukin 4

5D). From these experiments, we concluded that CAR T/NK-92 cells, on target-specific activation, produce considerable amounts of cytokines and chemokines that collectively are potent stimulators of PD-L1 expression and can be responsible for the observed self-amplifying cytotoxic activity of PD-L1–CAR-bearing cells. Since PD-L1–CAR T cells rapidly eliminate the target cells with induced PD-L1 expression cells (online supplemental figure 6A-C), we examined the full extent of bystander PD-L1 induction using HER-2–CAR T cells incubated with HER-2-positive

target tumor. As shown in figure 5D (left panel), we observed a potent induction of PD-L1 expression on MCF-7 cells on incubation with HER-2–CAR T cells and an even stronger induction in the SKBR-3 cell line (figure 5D, right panel), most probably due to the higher abundance of HER-2 in the latter (online supplemental figure 6D).

In summary, we conclude that the induction of PD-L1 occurring during the incubation of target cells with CAR T cells is a universal phenomenon. Moreover, PD-L1–CAR T cells can act on their targets in a 'rolling snowball' mode. The cytotoxic effects against PD-L1^{low} targets can be self-amplifying and spreading to the surroundings due to CAR T-induced, in a juxtacrine and/or paracrine manner, increase of PD-L1 molecule expression on the surface of the target and bystander cells, respectively. To the best of our knowledge, such a self-amplification phenomenon is unique among the CAR-based strategies. From our understanding, it can act as a double-edged sword. A positive consequence for the therapy of tumors would be a markedly expanded potential spectrum of malignancies targeted with the PD-L1–CAR-based therapies. However, since the PD-L1^{low} cells can become targets for PD-L1–CAR cells, it becomes important to investigate whether such therapies are toxic against non-malignant cells.

Expression of PD-L1 in non-malignant cells

To determine the cytotoxicity of PD-L1–CAR against normal cells, we have assessed PD-L1 protein presence in steady state in non-malignant mammary cell lines (spontaneously immortalized MCF-10A cell line and telomerase-immortalized human mammary epithelial cells (HMEC)), primary bone marrow-derived mesenchymal stromal cells (BM-MSC), and non-malignant embryonic kidney HEK-293T cell line. Both flow cytometry (figure 6A, left panels) and western blotting (figure 6A, right panels) demonstrated the low but detectable steady-state PD-L1 protein levels in MCF-10A and HMEC. For BM-MSCs, PD-L1 signal in western blotting was higher, but in flow cytometry, the surface PD-L1 expression remained below the level of detection. This indicates that in the steady state of BM-MSC, the PD-L1 molecule is located predominantly in the intracellular/cytoplasmic compartment(s). Lastly, no presence of PD-L1 protein was detected in HEK-293T cells by either of the abovementioned methods. Moreover, while MCF-10A, HMEC, and BM-MSC cells responded to the incubation with IFNγ by a significant increase in PD-L1 expression, HEK293T cells remained PD-L1 negative (figure 6A) on stimulation with IFNγ. Notably, the resistance of HEK293T cells to IFNγ-induced expression of PD-L1 is in accordance with the previous publication by Mimura *et al*.[15] Finally, when all four cell types were incubated with the conditioned supernatants from CAR T cocultures with target MDA-MB-231 cells, the MCF-10A (figure 6B, left panel), HMEC (figure 6C, left panel), and BM-MSC (figure 6D, left panel) cells showed a spectacular increase in PD-L1 expression level, whereas the HEK293T cells, again, remained >99% PD-L1 negative (figure 6E, left panel).

The activity of PD-L1–CAR effector cells against non-malignant cells

The surface presence of PD-L1, either in steady state or induced, on the majority of tested non-malignant cells suggested that these cells can also become targets to PD-L1–CAR-mediated cytotoxicity, either immediate or due to the self-amplification phenomenon described above. Indeed, both MCF-10A and HMEC cells were eliminated by PD-L1–CAR T cells in an E:T ratio-dependent manner, as presented in figure 6B,C (right panels), respectively. Moreover, when the BM-MSC cells were incubated with PD-L1–CAR T (RTCA assay, figure 6D, right panel) or PD-L1–CAR–NK-92 (fluorescent microscopy with the fluorescent probe detecting activation of caspase 3/7, online supplemental figure 7A), a potent cytotoxic effect was observed. Interestingly again, the steady-state BM-MSCs were eliminated by the PD-L1–CAR-bearing effector cells with latency as compared with the BM-MSC preincubated with IFNγ. This delay most probably results from the time-dependent induction of PD-L1 expression by the cytokines secreted by the CAR T cells. Simultaneously, the HEK293T cells, which were not prone to the cytokine-induced expression of PD-L1 (figure 6E, left panel), were almost completely resistant to the cytotoxic effects of PD-L1–CAR T cells, even in the high E:T (ie, 5:1) ratio (luminescence-based test, figure 6E, right panel, green bars). In order to exclude the possibility that these cells possess an impairment in response to the cytotoxic effect of immune effector cells, we have generated a PD-L1-overexpressing derivative of HEK293T cells (online supplemental figure 7B). These HEK293T–PD-L1 cells were readily killed by PD-L1–CAR T cells, while the empty-vector controls retained the resistance to cellular cytotoxicity (figure 6E, right panel, red bars), similar to the parental HEK293T cells. This substantiates the notion that the self-amplification effect of anti-PD-L1–CAR relies strictly on the capability of the target cells to increase PD-L1 expression in response to the cytokines released from the effector cells.

Sequential killing by HER2–CAR T and PD-L1–CAR T combination

Having identified the phenomenon of PD-L1 induction in target cells following the interaction with PD-L1–CAR effector cells, we have decided to interrogate the strategy to increase the precision of PD-L1–CAR-based therapy and the susceptibility of the tumor to this CAR. Specifically, the results described above (figure 5D) brought us to the conclusion that solid-tumor targeted CAR T cells (eg, HER-2–CAR T cells) can 'prepare' (ie, sensitize by increasing PD-L1 expression) cancer cells and TME to the actions of PD-L1–CAR T cells. To test this hypothesis, we carried out sequential, combined incubations of MCF-7 cells with HER-2–CAR T and/or PD-L1–CAR T cells (please refer to figure 7A for the experiment

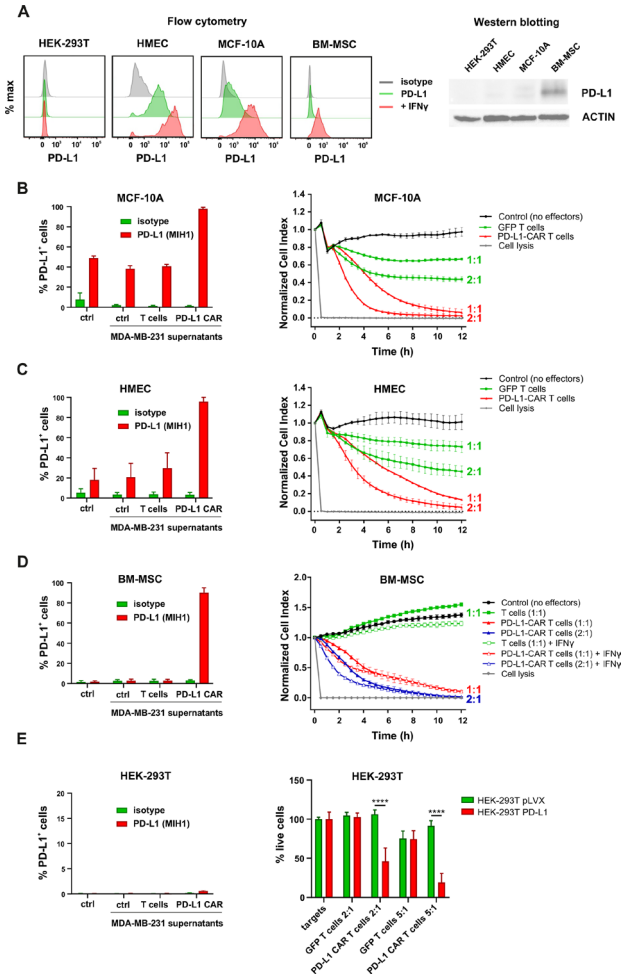

Figure 6 Expression of PD-L1 and PD-L1–CAR T mediated cytotoxicity in non-malignant cells. (A) IFNγ induced expression of PD-L1 on HEK293T cell line derived from human embryonic kidney cells and non-malignant cells (HMEC, MCF-10A, and bone marrow-derived mesenchymal stem cells (BM-MSC)) assessed by flow cytometry as presented on the left panel. PD-L1 staining was performed using anti-PD-L1 antibody (clone MIH1). The representative western blot analysis of PD-L1 expression in human embryonic kidney HEK293T cells and non-malignant mammary epithelial HMEC and MCF10A cells, and BM-MSC (right panel). β-actin was used as a loading control. The experiment was repeated three times. (B) PD-L1 expression induced on MCF-10A cells by activated CAR T cells (left panel) and RTCA-monitored cytotoxic activity of PD-L1 CAR T cells toward MCF-10A cells (right panel). The control (only medium) and conditioned supernatants from the 24 hours coincubation cultures in the presence of control (unmodified) T cells or PD-L1–CAR T cells with the target MDA-MB-231 cells were transferred onto the cultures of MCF-10A cell line and incubated for 48 hours. Next, PD-L1 surface presence was assessed by flow cytometry using anti-PD-L1 antibody (clone MIH1). Cytotoxic activity of PD-L1–CAR T cells against MCF-10A non-malignant cell line was measured by impedance analysis at the E:T ratios of 1:1 and 2:1. Samples were internally normalized for the cell index value measured before PD-L1–CAR T cells addition (Normalized Cell Index plots). The experiment was performed in duplicates three times. (C) PD-L1 expression induced on HMEC cells by activated CAR T cells (left panel) and RTCA-monitored cytotoxic activity of PD-L1 CAR T cells toward HMEC cells (right panel) was performed as described for (B). (D) PD-L1 expression induced on BM-MSC cells by activated CAR T cells (left panel) and cytotoxic activity of PD-L1–CAR T cells against BM-MSCs in the absence or presence of 25 ng/mL IFNγ was measured by impedance analysis at the E:T ratios of 1:1 and 2:1 (right panel). The experiment was performed in duplicates at least two times. (E) PD-L1 expression induced on HEK-293T cells by activated CAR T cells (left panel) and the killing potential of control (GFP-modified T cells) and PD-L1–CAR T cells against non-malignant human embryonic kidney cells HEK-293T pLVX (PD-L1$^{low/null}$) and HEK-293T PD-L1 (PD-L1^{+}) was determined by luciferase-based killing assay following coculture of target and effector cells for 18 hours at different E:T ratios (right panel). The assay was repeated twice in triplicate and the results shown are representative of one experiment. CAR, chimeric antigen receptor; HMEC, human mammary epithelial cells, PD-L1, programmed death-ligand 1, IFNγ, interferon γ, GFP, green fluorescent protein, RTCA, real-time cell analysis.

schematic). Notably, we have used suboptimal, regarding the cytotoxic activity (online supplemental figure 6C), E:T ratio of HER-2–CAR T cells in order to avoid the high background cytotoxicity. Importantly, HER-2–CAR T cells in such E:T ratio successfully induced PD-L1 expression in a considerable percentage of target MCF-7 cells within 6 hours (figure 7B, red bars), marking these cells for PD-L1–CAR T targeting. Indeed, we observed that target

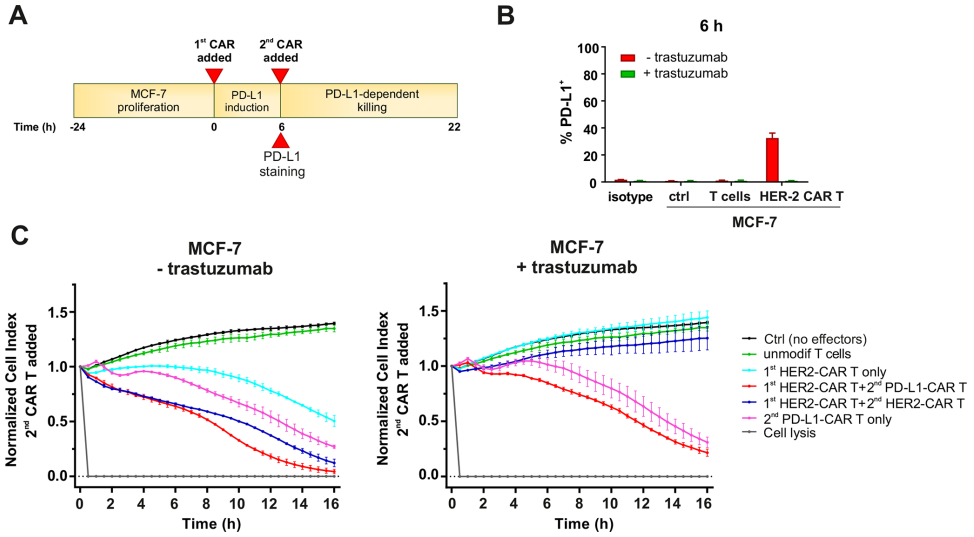

Figure 7 Sequential killing by HER2–CAR T and PD-L1–CAR T combination. (A) The schematic diagram of the sequential killing experiment. MCF-7 cells were left to proliferate for 24 hours. Next, MCF-7 cells were incubated with medium, HER-2–CAR or PD-L1–CAR T cells for 6 hours to induce PD-L1 expression on MCF-7 surface. Trastuzumab at the concentration 100 µg/mL was used as a blocking antibody for HER-2 antigen. After 6 hours, a fresh portion of the medium, PD-L1–CAR or HER-2–CAR T cells were added, followed by measuring the killing potential for the next 16 hours. Arrow indicates the time of surface staining of PD-L1 by flow cytometry performed in the parallel experiment (B). (B) PD-L1 expression induced on MCF-7 cells after 6 hours of coincubation with HER-2–CAR T cells in presence or absence of 100 µg/mL trastuzumab. PD-L1 surface presence was assessed using an anti-PD-L1 antibody (clone MIH1) by flow cytometry. The experiment was repeated in duplicates two times. (C) The sequential killing of MCF-7 cell lines was measured by impedance analysis in RTCA assay. CAR T cells were added at the E:T ratio of 0.5:1 with or without 100 µg/mL trastuzumab supplementation. Representative mean impedance curves from two wells after the addition of the second portion of PD-L1–CAR T cells are shown. The experiment was repeated in duplicates at least two times. CAR, chimeric antigen receptor, PD-L1, programmed death-ligand 1, HER2, human epidermal growth factor receptor 2, RTCA, real-time cell analysis.

cells preincubated with HER-2–CAR T cells responded to PD-L1–CAR T cells without delay, while when PD-L1–CAR T cells were added to cells without prior HER-2–CAR T treatment, the 4-6-hour delay in cytotoxic response was present again (figure 7C, left-hand panel). This strongly indicates the validity of such an approach. Moreover, the delay in cytotoxicity of PD-L1–CAR T cells against MCF-7 cells was retained when the experiment was carried in the presence of trastuzumab (figure 7C, right panel), that is, the antibody competitively blocking the binding of HER-2–CAR to its target and subsequent induction of PD-L1 (figure 7B, green bars). From these experiments, we conclude that PD-L1–CAR can play a supportive role for other solid tumor-targeted CARs by eliminating the reactive PD-L1-positive cells, if applied sequentially after the tumor-specific CAR, even in a low E:T ratio. In such settings, PD-L1–CAR T cells would eradicate cancer cells, but additionally may also kill the TME cells (such as tumor-associated macrophages), if those were responding to the first CAR-based treatment by upregulating PD-L1 immune checkpoint on their surface. It should be noted, that in such an approach, the HER-2–CAR T cells would be also eliminated by sequentially added PD-L1–CAR T cells, but this phenomenon can, in theory, be avoided by knocking out (eg, by CRISPR/Cas9 approach) *CD274* gene in HER2–CAR T cells. This subject warrants further investigations.

DISCUSSION

PD-L1 immune checkpoint molecule is an attractive target for the immunotherapeutic strategies against a range of human malignancies, with a special emphasis on solid tumors.[2 16] This is due to the fact that not only PD-L1 molecule, expressed on a significant number of cancer cells, but also other cells within the TME, are documented to inhibit the antitumor function of immune effector cells. An obvious advantage of the CAR-based approach over the inhibition of the PD-L1/PD-1 axis by the most of the anti-PD-L1 monoclonal antibodies[17] is a permanent effect of the physical elimination of the PD-L1-expressing target cells within TME. Therefore, it can be expected that PD-L1–CAR cells could not only be used for killing the PD-L1^{high} malignant cells per se but may also induce the reshaping of TME by eradication of its immunosuppressive PD-L1-positive cellular components. The same holds true for the CAR (other than anti-PD-L1 CAR) T cells plus anti-PD-L1 antibody combination approach in the solid tumors, although the activity of CAR T cells against the malignant cells can indeed be increased by the anti-PD-L1 antibodies.[18]

However, an important question is whether the PD-L1$^{low/null}$ tumors should be disregarded for the PD-L1–CAR T-based/NK-based treatment, as initially suggested.[19] We addressed this question in our study by investigating the responsiveness of initially PD-L1$^{low/null}$ targets to

the PD-L1–CAR-mediated cytotoxicity. In this study, we describe a potent and time-dependent ability of activated immune effector cells bearing PD-L1–CAR to induce the expression of PD-L1 molecule on the surface of a number of cell types, either in a juxtracrine or paracrine manner. This can make the initially PD-L1^{low} cells, such as MCF-7 cell line, vulnerable to the PD-L1–CAR-mediated cytotoxicity. In this context, our results are in accordance with the work by Robbins *et al*, which demonstrated that the effectiveness of PD-L1–CAR-bearing effector cells can be significantly amplified following the preincubation of cancer cells with IFNγ.[7]

Moreover, it has already been widely documented by others that the expression of PD-L1 can be potently induced by various proinflammatory agents, such as TNFα or IFNγ (reviewed by Ribas)[2] or direct contact with immune effector cells.[20] Hereby, we report a massive induction of PD-L1 as a consequence of antigen-specific CAR activation and production of cytokines. Activated immune effector cells are well-known sources of a broad set of proinflammatory factors, which we show in the current work to synergistically upregulate surface PD-L1 expression to the highest levels, as compared with IFNγ only treatment (figure 5D). Similar to our observations, trastuzumab (anti-HER2 antibody) was shown to upregulate PD-L1 level in HER2-overexpressing human breast cancer cells by stimulating human peripheral blood mononuclear cells to release IFNγ.[21]

Importantly, the effect of amplifying the expression of PD-L1 on the target or bystander cells by the activated CAR-bearing immune effector cells can have both positive and negative consequences. We consider this self-amplification phenomenon, exceptional in comparison with other CAR-based therapies, to be vital for further studies on this CAR, as it may significantly broaden the spectrum of potential targets for the PD-L1–CAR-based strategies. Our results obtained from the experiments with macrophages (figure 5B), a classical constituent of TME, suggest a potential paracrine effect of target-stimulated CAR T cells. This would additionally broaden the cytotoxic reaction of PD-L1-CAR cells toward the tumor stroma cells adjacent to the malignant cells, even if the stromal cells were initially PD-L1$^{low/null}$.

The PD-L1 amplification phenomenon by the activated CAR effector cells may have a broader effect and influence the efficacy of various CAR-based approaches. Given the role of PD-L1 molecule as a negative regulator of the T-cell immune response, upregulation of PD-L1 following the treatment with CAR T cells may function as a mechanism of resistance to CAR-based strategies employed against solid tumors. This finding encourages further investigation of the advantage of adding anti-PD-1/PD-L1 therapy to CAR-based treatments (reviewed by Kosti *et al*)[22], especially in patients with low constitutive PD-L1 expression. Interestingly, the combination of high-affinity PD-L1-CAR NK cells withthe IL-15 superagonist and anti-PD-1 antibody has been already demonstrated by others to have superior tumor growth control of engrafted oral cavity squamous carcinoma tumors in mice.[23] The effect of amplifying the PD-L1 expression can also serve as a stimulus for incorporating the PD-L1–CAR into combinations with other CAR-based strategies. Indeed, in this work, we provide a proof of concept for sensitizing the breast cancer cells to PD-L1–CAR T cells by their prior incubation with HER-2–CAR T cells (figure 7). Therefore, our data suggest that due to the effect of reactive expression of PD-L1 on target cells after their incubation with CAR T cells, the PD-L1–CAR T cells may be used to amplify the effectiveness of alternative CARs applied in solid tumors treatment. Surprisingly, however, when PD-L1–CAR T cells were used in addition to the mesothelin-targeting CAR T cells in the previous work by Qin *et al*,[24] an antagonistic interaction was observed. The explanation relies on the fact that PD-L1–CAR T cells can induce fratricide effects against other activated CAR T cells, as the latter start expressing PD-L1 on their surface following recognition of the target. Indeed, we report a similar phenomenon in this work, that is, the activated CD19–CAR T cells readily expressed PD-L1 on their surface, while the PD-L1–CAR T cells remained PD-L1^{null} following activation (online supplemental figure 3B), which might be attributed to masking PD-L1 by PD-L1–CAR on the cell surface, as suggested previously,[24] or, alternatively, elimination of the T-cell subpopulation with inducible PD-L1 expression by those PD-L1–CAR T cells, which do not express PD-L1. We respond to this question in our study, by presenting that PD-L1–CAR T cells lose the capability of expressing PD-L1 protein (online supplemental figure 3D); however, they retain the expression of PD-L1 mRNA on induction by activatory stimulus (online supplemental figure 3E). The exact mechanism of this phenomenon warrants further investigations.

These observations imply that in combinatory approaches involving PD-L1–CAR T cells, the expression of PD-L1 on other CAR T cells should be prevented, for example, by genetic KO of the *CD274* gene, RNAi-mediated knockdown, or in vitro preincubation of other CAR T cells with PD-L1–CAR cells. An additional benefit from suppressing the PD-L1 molecule in CAR T cells can be related to the fact that PD-L1 engagement on T cells has been shown to promote the suppression of neighboring macrophages and effector T cells in cancer.[24] Moreover, PD-L1 expression on T cells has been very recently demonstrated to play an important role in the suppression of T cells, and PD-L1^{+} T cells have diverse tolerogenic effects on tumor immunity.[25] Thus, removing the ability of PD-L1 expression from the CAR T cells would not only protect them from PD-L1–CAR T cells used in combination, but also might amplify their effectiveness per se. This issue warrants further investigation.

The negative consequences of the PD-L1 amplification phenomenon are related to the safety issues of this strategy in clinical settings. PD-L1 molecule is involved in peripheral immune self-tolerance toward numerous healthy tissues, with the highest steady-state expression level not only in the placenta but also in vital organs such as lungs, intestine, or heart. Accordingly, the risk of inducing the immune-related adverse effects by tampering with the PD-L1 functions is clearly demonstrated in patients treated with anti-PD-L1 checkpoint

blockers (reviewed by Choi and Lee).[26] Therefore, it is of the utmost importance to properly assess the potential toxicities of PD-L1–CAR-based strategies against the non-malignant cells. In our work, we have used four non-malignant types of cells (both established cell lines and primary cells) to investigate the toxicity of PD-L1–CAR T/NK-92 cells. Our data show that PD-L1–CAR T cells can exhibit potent cytotoxicity against non-malignant cells, as long as those express PD-L1 molecule in steady state (MCF-10A and HMEC cells) or in response to the proinflammatory stimulus (BM-MSC). The only cell line resistant to the PD-L1–CAR-mediated toxicity was HEK293T, which was PD-L1^{null} initially and remained refractory to the induction of PD-L1 expression either by IFNγ or the conditioned medium derived from cultures of activated CAR T cells. Importantly, the exogenous expression of PD-L1 on HEK293T cells made them sensitive to the PD-L1–CAR T-mediated toxicity, eliminating the possibility that these cells were resistant to cell-mediated cytotoxicity in general.

The sensitivity of non-malignant cells to PD-L1–CAR-mediated toxicity suggests that PD-L1–CAR-based therapies should be evaluated with extreme caution while applied in humans. This notion is especially highlighted by the fact that the clinical trial in patients with advanced lung cancer involving PD-L1–CAR T cells (ClinicalTrials.gov Identifier: NCT03330834) was recently terminated due to serious, however, resolved on tocilizumab and steroids treatment, adverse effects after one patient received the treatment. In this regard, previous groups testing PD-L1–CAR T cells in human-to-mouse xenotransplantation tumor models reported no apparent generalized toxicity of the therapy in mice, even though atezolizumab-based CARs are expected to be cross-reactive with mouse PD-L1. It must be underscored, however, that human T cells can induce immense graft-versus-host reaction in the mouse body,[27] which can significantly mask the delayed toxicity of PD-L1–CAR. Therefore, the preclinical safety studies with PD-L1–CAR must be appropriately designed in order to identify the potentially severe on-target, off-tumor adverse effects. In the case of detecting the generalized toxicity of PD-L1–CAR-based therapies, further studies must be conducted in order to optimize the precision of these strategies toward malignant burden and minimize the risk of the toxicities to the healthy tissues. Theoretically, that might be achieved by controlled/inducible expression of PD-L1–CAR, such as hypoxia-sensing system,[28] transient expression by mRNA electroporation, or application of agents neutralizing proinflammatory factors[21] and thus preventing the PD-L1 self-amplification effect. Also, it seems plausible that since NK cells are not so abundantly producing proinflammatory cytokines, modifications of NK cells and NK-92 cell line, instead of T cells, would be a more appropriate design for PD-L1–CAR to avoid the rolling snowball effect and off-tumor toxicity. Indeed, PD-L1–CAR ha (high affinity) NK cells were already shown by others to be effective and safe in the treatment of immunodeficient mice bearing human head and neck cancer xenograft tumors,[7] as well as triple-negative breast cancer (TNBC), lung or bladder tumors.[23] However, the results presented in current work, as presented in figure 5C, indicate that the pattern of cytokines produced by target-activated CAR–NK-92 can be still sufficient for induction of PD-L1 on the target and bystander cells. This subject requires further assessment.

In summary, we demonstrate the efficacy of PD-L1–CAR T/NK/NK-92 cells against a model of triple-negative breast cancer intrinsically expressing high levels of PD-L1.[29] Our work corroborates the notion that PD-L1 is an attractive target for prospective CAR-based anticancer therapies and could be applied in a considerable percentage of malignancies of various histopathological types to directly eliminate tumor cells and TME cells expressing PD-L1 on their surface.

This study also brings new information on the potential application of PD-L1 CAR against PD-L1$^{low/null}$ tumors, as long as they respond to proinflammatory cytokines by upregulation of PD-L1 on the cellular surface. Also, our results imply that targeting PD-L1 raises the considerable risk of on-target, off-tumor reactivity of the PD-L1–CAR-bearing effector cells toward non-malignant tissue and help to explain the mechanisms of potential toxicities of PD-L1–CAR T cells. We suggest the need to find safer approaches using the PD-L1–CAR-bearing effector cells and propose an example strategy for PD-L1–CAR as an agent supporting and amplifying the effectiveness of other CARs when administered sequentially. Collectively, based on our observations, we assume that the potential targets for CAR-based therapies should be regularly analyzed for their inducibility by proinflammatory cytokines, as this may change the specificity and safety spectrum and finally change the validity of a given target. We believe that the information presented in this study may change the future approaches aimed at the development of successful CAR-based therapies against solid tumors.

Author affiliations
[1]Department of Clinical Immunology, Medical University of Warsaw, Warszawa, Mazowieckie, Poland
[2]Laboratory of Immunology, Mossakowski Medical Research Institute, Polish Academy of Sciences, Warsaw, Poland
[3]Department of Immunology, Medical University of Warsaw, Warszawa, Poland
[4]Postgraduate School of Molecular Medicine, Medical University of Warsaw, Warsaw, Poland
[5]Laboratory for Cellular and Genetic Therapies, Medical University of Warsaw, Warsaw, Poland
[6]Department of Immunology, Transplantology and Internal Diseases, Medical University of Warsaw, Warszawa, Poland
[7]Doctoral School, Medical University of Warsaw, Warsaw, Poland
[8]Doctoral School of Translational Medicine, Centre of Postgraduate Medical Education, Warsaw, Poland
[9]Department of Bioinformatics, Institute of Biochemistry and Biophysics, Polish Academy of Sciences, Warsaw, Poland
[10]Department of Cancer Immunology, Radiumhospitalet, Oslo, Norway
[11]Department of Cellular Therapy, Oslo University Hospital, Oslo, Norway
[12]Department of Regenerative Medicine, The Maria Sklodowska-Curie National Research Institute of Oncology, Warsaw, Poland

Correction notice This article has been updated since it was first published. The funding statement has been amended.

Acknowledgements The authors would like to acknowledge Dr Iwona Baranowska and Mrs Ewa Pieta for routine peripheral blood mononuclear cells (PBMC) preparation and technical assistance. The authors thank Jon Amund Kyte (OUS, Norway) for the SFG-CD19-CAR construct (originally obtained as a kind gift from Martin Pule, UCL, UK).

Contributors MB: conceptualization, investigation, data curation, visualization, methodology, formal analysis, and writing—review and editing. AG-J: conceptualization, investigation, visualization, data curation, methodology, formal analysis, resources, and writing—review and editing. KM: conceptualization, investigation, visualization, methodology, formal analysis, and writing—review and editing. AB, AM, and AG: investigation, visualization, methodology, data curation, and formal analysis. AZ, KS, and SE: investigation, methodology, and data curation. KR: investigation, methodology, data curation, visualization, and formal analysis. MKrawczyk and MKlopotowska: investigation, methodology, data curation, and formal analysis. ZP: investigation and methodology. LP: resources and supervision. K-JM: conceptualization and writing—review and editing. MW: conceptualization, resources, supervision, funding acquisition, visualization, project administration, and writing—review and editing. RZ: conceptualization, resources, supervision, funding acquisition, project administration, writing—original draft, responsible for the overall content as guarantor, accepts full responsibility for the finished work and the conduct of the study, had access to the data, and controlled the decision to publish.

Funding The work was supported by the grants from the National Science Centre, Poland (2016/23/B/NZ6/02535, RZ; 2019/35/D/NZ6/03073, AG-J, and 2019/33/B/NZ6/02503, MB), the Polpharma Scientific Foundation (5FPOL8, AG-J), the European Research Council (805038/STIMUNO/ERC-2018-STG, MW), the Medical Research Agency (2020/ABM/04/00002), and the Ministry of Science and Higher Education within 'Regional Initiative of Excellence' (013/RID/2018/19, 2019–2022).

Competing interests K-JM is a consultant at Fate Therapeutics and a member of the SAB at Vycellix.

Patient consent for publication Not applicable.

Ethics approval This study does not involve human participants.

Provenance and peer review Not commissioned; externally peer reviewed.

Data availability statement Data sharing not applicable as no datasets were generated and/or analyzed for this study. All data relevant to the study are included in the article or uploaded as supplementary information.

ORCID iDs
Magdalena Winiarska http://orcid.org/0000-0001-5605-3329
Radoslaw Zagozdzon http://orcid.org/0000-0002-7957-2372

REFERENCES

1 Yang Y, Li C-W, Chan L-C, *et al*. Exosomal PD-L1 harbors active defense function to suppress T cell killing of breast cancer cells and promote tumor growth. *Cell Res* 2018;28:862–4.
2 Ribas A. Adaptive immune resistance: how cancer protects from immune attack. *Cancer Discov* 2015;5:915–9.
3 Parra ER, Villalobos P, Rodriguez-Canales J. The multiple faces of programmed cell death ligand 1 expression in malignant and nonmalignant cells. *Appl Immunohistochem Mol Morphol* 2019;27:287–94.
4 Tang J, Hubbard-Lucey VM, Pearce L, *et al*. The global landscape of cancer cell therapy. *Nat Rev Drug Discov* 2018;17:465–6.10.1038/nrd.2018.74
5 Yoon D, Osborn M, Tolar J, *et al*. Incorporation of immune checkpoint blockade into chimeric antigen receptor T cells (CAR-Ts): combination or built-in CAR-T. *Int J Mol Sci* 2018;19:340.
6 Xie YJ, Dougan M, Jailkhani N, *et al*. Nanobody-Based CAR T cells that target the tumor microenvironment inhibit the growth of solid tumors in immunocompetent mice. *Proc Natl Acad Sci U S A* 2019;116:7624–31.
7 Robbins Y, Greene S, Friedman J, *et al*. Tumor control via targeting PD-L1 with chimeric antigen receptor modified NK cells. *Elife* 2020;9:9.
8 Qin W, Hu L, Zhang X, *et al*. The diverse function of PD-1/PD-L pathway beyond cancer. *Front Immunol* 2019;10:2298.
9 Li S, Chen L, Jiang J. Role of programmed cell death ligand-1 expression on prognostic and overall survival of breast cancer: a systematic review and meta-analysis. *Medicine* 2019;98:e15201.
10 Kim HM, Lee J, Koo JS. Clinicopathological and prognostic significance of programmed death ligand-1 expression in breast cancer: a meta-analysis. *BMC Cancer* 2017;17:690.
11 Matikas A, Zerdes I, Lövrot J, *et al*. Prognostic implications of PD-L1 expression in breast cancer: systematic review and meta-analysis of immunohistochemistry and pooled analysis of transcriptomic data. *Clin Cancer Res* 2019;25:5717–26.
12 Zhai Q, Fan J, Lin Q, *et al*. Tumor stromal type is associated with stromal PD-L1 expression and predicts outcomes in breast cancer. *PLoS One* 2019;14:e0223325.
13 Wagner J, Rapsomaniki MA, Chevrier S, *et al*. A single-cell atlas of the tumor and immune ecosystem of human breast cancer. *Cell* 2019;177:1330–45.
14 Cassetta L, Kitamura T. Targeting tumor-associated macrophages as a potential strategy to enhance the response to immune checkpoint inhibitors. *Front Cell Dev Biol* 2018;6:38.
15 Mimura K, Teh JL, Okayama H, *et al*. Pd-L1 expression is mainly regulated by interferon gamma associated with JAK-STAT pathway in gastric cancer. *Cancer Sci* 2018;109:43–53.
16 Marhelava K, Pilch Z, Bajor M, *et al*. Targeting negative and positive immune checkpoints with monoclonal antibodies in therapy of cancer. *Cancers* 2019;11:1756.
17 Lee YJ, Lee JB, Ha S-J, *et al*. Clinical perspectives to overcome acquired resistance to Anti-Programmed death-1 and Anti-Programmed death ligand-1 therapy in non-small cell lung cancer. *Mol Cells* 2021;44:363–73.
18 Grosser R, Cherkassky L, Chintala N, *et al*. Combination immunotherapy with CAR T cells and checkpoint blockade for the treatment of solid tumors. *Cancer Cell* 2019;36:471–82.
19 Xie J, Zhou Z, Jiao S, *et al*. Construction of an anti-programmed death-ligand 1 chimeric antigen receptor and determination of its antitumor function with transduced cells. *Oncol Lett* 2018;16:157–66.
20 Liu G, Zhang Q, Li D, *et al*. Pd-1 silencing improves anti-tumor activities of human mesothelin-targeted CAR T cells. *Hum Immunol* 2021;82:130–8.
21 Chaganty BKR, Qiu S, Gest A, *et al*. Trastuzumab upregulates PD-L1 as a potential mechanism of trastuzumab resistance through engagement of immune effector cells and stimulation of IFNγ secretion. *Cancer Lett* 2018;430:47–56.
22 Kosti P, Maher J, Arnold JN. Perspectives on chimeric antigen receptor T-cell immunotherapy for solid tumors. *Front Immunol* 2018;9:1104.
23 Fabian KP, Padget MR, Donahue RN, *et al*. Pd-L1 targeting high-affinity NK (t-haNK) cells induce direct antitumor effects and target suppressive MDSC populations. *J Immunother Cancer* 2020;8:e000450.
24 Qin L, Zhao R, Chen D, *et al*. Chimeric antigen receptor T cells targeting PD-L1 suppress tumor growth. *Biomark Res* 2020;8:19.
25 Diskin B, Adam S, Cassini MF, *et al*. Pd-L1 engagement on T cells promotes self-tolerance and suppression of neighboring macrophages and effector T cells in cancer. *Nat Immunol* 2020;21:442–54.
26 Choi J, Lee SY. Clinical characteristics and treatment of immune-related adverse events of immune checkpoint inhibitors. *Immune Netw* 2020;20:e9.
27 Ito R, Katano I, Kawai K, *et al*. A Novel Xenogeneic Graft-Versus-Host Disease Model for Investigating the Pathological Role of Human CD4 $^{+}$ or CD8 $^{+}$ T Cells Using Immunodeficient NOG Mice. *Am J Transplant* 2017;17:1216–28.
28 Kosti P, Opzoomer JW, Larios-Martinez KI, *et al*. Hypoxia-sensing CAR T cells provide safety and efficacy in treating solid tumors. *Cell Rep Med* 2021;2:100227.
29 Liu L, Shen Y, Zhu X, *et al*. Erα is a negative regulator of PD-L1 gene transcription in breast cancer. *Biochem Biophys Res Commun* 2018;505:157–61.

Correction: *PD-L1 CAR effector cells induce self-amplifying cytotoxic effects against target cells*

Bajor M, Graczyk-Jarzynka A, Marhelava K, *et al*. PD-L1 CAR effector cells induce self-amplifying cytotoxic effects against target cells. *J ImmunoTher Cancer* 2022;10:e002500. doi: 10.1136/jitc-2021-002500

The funding statement for this paper was incorrect. The funding statement has been updated to:

The work was supported by the grants from the National Science Centre, Poland (2016/23/B/NZ6/02535, RZ; 2019/35/D/NZ6/03073, AG-J, and 2019/33/B/NZ6/02503, MB), the Polpharma Scientific Foundation (5FPOL8, AG-J), the European Research Council (805038/STIMUNO/ERC-2018-STG, MW), the Medical Research Agency (2020/ABM/04/00002), and the Ministry of Science and Higher Education within 'Regional Initiative of Excellence' (013/RID/2018/19, 2019–2022).

J Immunother Cancer 2022;**10**:e002500corr1. doi:10.1136/jitc-2021-002500corr1

Supplementary data.

Materials and methods.

Cell lines

Human breast carcinoma cell lines: MCF-7 (RRID:CVCL_0031), ZR-75-1 (RRID:CVCL_0588), T47D (RRID:CVCL_0553), MDA-MB-231 (RRID:CVCL_0062), HCC-1806 (RRID:CVCL_1258), SKBR-3 (RRID:CVCL_0033), and a non-malignant immortalized mammary cell line MCF-10A (RRID:CVCL_0598) were purchased from the European Collection of Cell Cultures (Wiltshire, UK). Cells were cultured in DMEM (ZR-75-1, T47D) or RPMI-1640 (MCF-7, MDA-MB-231, HCC-1806, and SKBR-3) media (Sigma-Aldrich, St Louis, MO, USA) supplemented with 10% fetal bovine serum (FBS) (Sigma-Aldrich), 2 mM L-glutamine (Sigma-Aldrich) and 1% antibiotics – penicillin/streptomycin (Sigma-Aldrich) in a humidified atmosphere containing 5% CO_2. Additionally, ZR-75-1 and T47D culture media were supplemented with 1nM β-estradiol (Sigma Aldrich). MCF-10A was cultured in mammary epithelial basal media (MEBM, Lonza) containing 0.4% bovine pituitary extract (BPE), 10 ng/ml human epidermal growth factor (hEGF), 5 µg/ml human insulin, 0.5 µg/ml hydrocortisone, 30 µg/ml gentamicin and 15 µg/ml amphotericin, and 100 ng/ml cholera toxin (Sigma-Aldrich). HMEC, primary human mammary epithelial cells, were purchased from Life Technologies (Carlsbad, CA). HMEC cells were cultured in HuMEC medium supplemented with epidermal growth factor, hydrocortisone, isoproterenol, transferrin, insulin, and 50 µg/ml bovine pituitary extract, according to manufacturer protocol (Life Technologies). HEK-293T (RRID:CVCL_0063) and Phoenix Ampho (RRID:CVCL_H716) cells were purchased from ATCC and were cultured in DMEM medium supplemented with 10% FBS. NK-92 cell line (RRID:CVCL_2142, a generous gift from Prof. Kerry Campbell) was maintained in X-VIVO™ 20 medium (Lonza) supplemented with 5% human serum (Sigma Aldrich). All the cell lines were authenticated in Eurofins Genomics, maintained through continuous passaging, and were confirmed to be free of contamination with Mycoplasma spp.

Peripheral blood mononuclear cells (PBMCs) and T cells selection

Peripheral blood mononuclear cells (PBMCs) were isolated from the whole blood by density gradient separation using Histopaque-1077 (Sigma-Aldrich, St Louis, MA, USA). The procedure was approved by the Local Bioethics Committee (approval number: AKBE/184/2018). After gradient centrifugation, PBMCs were seeded onto a 6-well plate at a cell density 1×10^6 per 1 ml in 3 ml RPMI-1640 medium supplemented with 10% FBS and 1% penicillin and streptomycin solution and stimulated using 2.4 µg/ml of phytohemagglutinin-L (PHA-L, Sigma Aldrich) for 3 days. After transduction, T cells were maintained in full RPMI-1640 medium supplemented with 100 U/ml IL-2 (Peprotech) and in the

presence of Dynabeads Human T-Activator CD3/CD28 (Thermo Fisher Scientific) at a bead-to-cell ratio of 1:5.

Macrophage isolation and differentiation

Freshly isolated PBMCs were suspended in RPMI-1640 (Biowest) and seeded onto 96-well, µCLEAR, black plates (Grainer, Ref No. 655090) at a cell density 3×10^5 per well in 100 µl. After 2 h of incubation in standard conditions (37°C, 5% CO_2, 95% humidity), the cells were washed once with PBS to remove unattached cells. Afterward, the remaining adherent cells considered as monocytes-enriched PBMCs were cultivated in the medium consisting of RPMI-1640 supplemented with 10% human serum (Sigma-Aldrich) and antibiotics (1% Penicillin-Streptomycin) in standard conditions. On the 3rd day of culture, the medium was changed, and the monocytes/macrophages either remained untreated or were stimulated with IFNγ (10 ng/ml) or a combination of IL-4 and IL-10 (10 ng/ml both). A fresh portion of the cytokines was added every other day.

Bone marrow collection

The bone marrow samples were obtained from patients after receiving their written consent. The procedure was approved by the Local Bioethics Committee (approval number: KB/115/2016). The bone marrow was collected during standard orthopedic surgeries, which required the opening of the bone marrow cavity.

Mesenchymal stromal cells isolation

Isolation was performed on the same day as the bone marrow was collected. The bone marrow, after mechanical disassociation, was washed with PBS and centrifuged at 300 × *g* for 5 min. The samples were then expanded in DMEM-LG growth medium (Dulbecco's modified Eagle's Medium with low glucose; Lonza) supplemented with 10% fetal calf serum (FCS, Lonza) and 1.5% antibiotic–antimycotic (AA) solution (Penicillin-streptomycin-amphotericin B, Invitrogen), seeded on BD Primaria^{TM} culture dishes (Becton Dickinson) and incubated under standard cell culture conditions (37°C, 5% CO_2, 95% humidity, and atmospheric oxygen concentration). After 4 days, non-adherent cells were removed, and first fibroblast-like adherent cells could be observed. When the colonies were well-formed (usually 7-10 days after isolation), the cells were passaged. Subsequent passages were performed when cells were reaching about 80% of confluence. After the third passage, the cells were frozen in liquid nitrogen. After thawing, cells underwent an identification process, which included differentiation assays and the analysis of cell surface antigen profile. The experiments were performed on the cells between 4 to 5 passage. The cells from different donors were always cultured separately.

Immunocytochemistry (ICC) analysis of PD-L1 and CD206 in macrophages

PD-L1 and CD206 expression in macrophages was assessed after 4 days of differentiation. T cells or PD-L1-CAR T cells conditioned supernatants from the 24-hour co-incubation with MDA-MB-231 cell line were placed instead of the medium for 48 h to assess the impact of these supernatants on induced PD-L1 expression. The cells were fixed with 4% paraformaldehyde (15 min, at 25°C). After washing, the cells were incubated with blocking buffer consisting of PBS with 2.5% normal donkey serum and 1% bovine serum albumin for 30 min (at 25°C), followed by overnight incubation (at 4°C) with primary goat anti-CD206 antibody (R&D Systems Cat# AF2534, RRID:AB_2063019, dilution 1:100) and primary mouse anti-PD-L1 antibody (Thermo Fisher Scientific Cat# 14-5983-82, RRID:AB_467784, dilution 1:100) solution in blocking buffer. Next, after washing, the cells were incubated with secondary antibodies (Alexa Fluor 647 donkey anti-goat IgG (H+L), Molecular Probes Cat# A-21447, RRID:AB_141844 and Alexa Fluor 488 donkey anti-mouse IgG (H+L) Molecular Probes Cat# A-21202, RRID:AB_141607) in blocking buffer (both 1:300) for 1 h at 25°C. Nuclei were stained with DAPI solution (20 ng/ml, for 4 min, at 25°C). The cells were visualized using automated imaging reader Cytation™ 1 (BioTek, Agilent). The images were analyzed using Gen5 3.04 software (BioTek, RRID:SCR_017317). The mean fluorescence intensity within secondary masks was measured. The secondary mask was designed around each DAPI stained nucleus (which constituted a primary mask).

Western blotting

Total protein lysates were prepared in the lysis buffer (50 mM Hepes, 150 mM NaCl, 5 mM EDTA, 1.0% (w/v) Triton X-100, 10% (v/v) glycerol, pH 7.4) supplemented with Complete Protease Inhibitor Cocktail (Roche Diagnostics, Basel, Switzerland). Protein concentration was determined using Pierce BCA Protein Assay Kit (ThermoFisher Scientific, Waltham, MA, USA) according to the manufacturer's instructions. Equal amounts of total protein lysates (20 µg) were separated in 12% (v/v) reducing SDS-polyacrylamide gel, then transferred onto nitrocellulose membranes, and blocked with 5% (w/v) nonfat dry milk in TBST (Tris-buffered saline, pH 7.4 and 0.05% (v/v) Tween-20) for 1 h at 25°C. Afterward, the membrane was incubated overnight at 4°C with the following primary antibodies: anti-PD-L1 (dilution 1:1000, Cell Signaling Technology Cat# 13684, RRID:AB_2687655) and anti-β-actin-HRP (1:40000 dilution, Sigma-Aldrich Cat# A3854, RRID:AB_262011). For the detection of specific protein bands, HRP-conjugated secondary antibodies were used. The blots were exposed to the Super Signal chemiluminescent substrate (Thermo Fisher Sci. Rockford, USA) and detected using ChemiDoc Imaging System (Bio-Rad ChemiDoc MP Imaging System, RRID:SCR_019037).

RNA isolation and quantitative real time PCR

Total RNA was isolated using RNeasy kit (Qiagen). RNA concentration was measured with NanoDrop 2000 spectrophotometer (Thermo Fischer Scientific, Waltham, MA, USA) and 500 ng of RNA was

reverse transcribed to complementary cDNA with the use of Superscript IV Reverse Transciptase kit and random hexamer primer (Thermo Fischer Scientific, Waltham, MA, USA) according to the manufacturer's instructions. Quantitative real-time PCR (qPCR) with LightCycler 480 SYBR Green I Master (Roche Diagnostics, Basel, Switzerland) was performed using LightCycler 480 II device (Roche Diagnostics, Basel, Switzerland) according to the manufacturer's recommendations in 20 µl final volume. In each PCR run, the samples were measured in duplicates. Primers used within the study are listed in the tble below:

F-PD-L1	5'-GCT GAA TTG GTC ATC CCA GAA-3'
R-PD-L1	5'-TTT CAC ATC CAT CAT TCT CCC TT-3'
F-SDHA	5'-GCA TTT GGC CTT TCT GAG GC-3'
R-SDHA	5'-CTC CAT GTT CCC CAG AGC AG-3'
F-TBP	5'-GCA CAG GAG CCA AGA GTG A-3'
R-TBP	5'-GTT GGT GGG TGA GCA CAA G-3'

Fluorescence Activated Cell Sorting

NK-92 cells from 80% confluent culture flasks were centrifuged and resuspended in PBS in a final concentration of 5 × 10^6 cells/ml. Then, the cells were transferred through a cell strainer to ensure separation of the cells. The sorting was performed according to surface CAR expression with FACS Aria III cell sorter (BD Biosciences, La Jolla, CA, USA).

CAR construction

PD-L1-targeting CAR synthesis was performed by Creative Biolabs, and the design was as follows: atezolizumab-based scFv sequence was combined with the CAR backbone consisting of full IgG4 hinge, CD28 transmembrane region, CD28, and CD3ζ signaling domains. Next, it was sub-cloned into the BamHI/SbfI restriction sites of the lentiviral transfer plasmid pSEW [1], thereby replacing the *gfp* gene. For some experiments (in vivo settings) atezolizumab based scFv was subcloned to CAR backbone with half IgG1 hinge, CD28 transmembrane region, CD28, and CD3ζ signaling domains and insereted into pSEW vector. HER2-CAR construct was designed from trastuzumab sequence (4D5, https://www.drugbank.ca/drugs/DB00072). Briefly, a degenerated DNA coding sequence of the scFv was ordered to Eurofins-MWG (Ebersberg, Germany) with a "light chain-$(G_3S)_3$ linker-heavy chain" structure as in [2]. The sequence was inserted into a second-generation CAR-backbone containing a CD8 hinge and transmembrane domain and a 4-1BB-CD3ζ signaling tail, as described in [3] and also, subsequentely, subcloned to pSEW lentiviral plasmid. For HER-2-CAR detection, a sequence coding a

truncated form of CD34 was inserted into the vector. Two CD19-CAR (FMC63 clone) constructs were used in this study, both, a kind gift from M. Pule (UCL, UK). SFG retroviral plasmid comprises the CD8 hinge and transmembrane domain, 41BB costimulatory domain, CD3ζ signaling domain, and rituximab recognized-RQR8 epitope for CAR detection. The second CD19-CAR construct comprises IgG1 half-hinge, CD28 transmembrane and co-stimulatory domain and CD3ζ and was inserted into pSEW plasmid.

Lentiviral and retroviral T cells modifications

PBMC isolated from buffy coats were seeded onto the 6-well plate at a cell density 1×10^6 cells per 1 ml in 3 ml RPMI full medium and stimulated using 2.4 ug/ml of PHA-L for 3 days. To produce control or CAR viral particles, HEK-293T cells were seeded at 10 cm plates – 4 plates per virus and transfected using a polyethyleneimine (PEI) transfection protocol to deliver a transfer plasmid with gene of interest simultaneously, VSV-G envelope expressing plasmid pMD2.G (a gift from Didier Trono; RRID:Addgene_12259) and lentiviral packaging plasmid psPAX2 (a gift from Didier Trono; RRID:Addgene_12260). After 48 h, the lentivirus-containing supernatant was harvested, filtered through a 0.45 µm pore size filter, and concentrated by overnight centrifugation at 2 500 × *g* at 4°C. The culture medium from the stimulated PMBC was replaced with concentrated lentiviral supernatant, and 4 µg/ml of polybrene (Sigma-Aldrich) was added. After 1 h of spinoculation round (2 000 × *g* at 32°C), the PMBC were kept in a humidified atmosphere containing 5% carbon dioxide (CO_2). The next day, the viral supernatant was replaced with the fresh portion of complete culture RPMI-1640 medium supplemented with 200 U/ml IL-2 (PeproTech) and Dynabeads Human T-Activator CD3/CD28 (Thermo Fisher Scientific) at a bead-to-cell ratio of 1:5). In the case of retroviral transduction, 2 x 10 cm plates of Phoenix Ampho cells were seeded per virus, and a gene of interest was co-transfected together with pHIT60 and pCOLT-GALV plasmids [4], a kind gift of Tuna Mutis (VUmc the Netherlands). Retroviral supernatant was collected, spun down at 500 x g for 5 min, and concentrated using Retro-X-Concentrator (Takara). Stimulated PBMC's were transferred on the 50 µg/ml Retronectin (Takara) coated plates, and concentrated retroviral supernatant was applied. After 1 h of spinoculation round (2 000 × *g* at 25°C), the PMBC were kept in a humidified atmosphere containing 5% carbon dioxide (CO_2). The spinoculation with the second batch of viral supernatant was repeated on the next day. Similar to lentiviral transduction, on the following day, the viral supernatant was replaced with the fresh portion of complete culture RPMI-1640 medium supplemented with 200 U/ml IL-2 (PeproTech) and Dynabeads Human T-Activator CD3/CD28 (Thermo Fisher Scientific) at a bead-to-cell ratio of 1:5. The CAR expression on the surface of the T cells was evaluated by flow cytometry 48-72 h after transduction.

Lentiviral modification of NK-92 cells

To produce control or PD-L1-CAR viral particles, HEK-293T cells were seeded at 10 cm plates – 4 plates per virus and transfected using a polyethyleneimine (PEI) transfection protocol to deliver a transfer plasmid with gene of interest simultaneously, VSV-G envelope expressing plasmid pMD2.G (RRID:Addgene_12259) and lentiviral packaging plasmid psPAX2 (RRID:Addgene_12260). After 48 h, the lentivirus-containing supernatant was harvested, filtered through a 0.45 µm pore size filter, and concentrated by overnight centrifugation at 2 500 × *g* at 4°C. The culture medium from the NK-92 cells was replaced with concentrated lentiviral supernatant supplemented with 15 µg/ml protamine sulfate and 6 µM BX-795. After 1 h of spinoculation (750 × *g* at 25°C), the NK-92 cells were kept in a humidified atmosphere containing 5% carbon dioxide (CO_2). The next day, the viral supernatant was replaced with the fresh portion of complete culture X-VIVO™ 20 medium (Lonza) supplemented with 200 U/ml IL-2 (PeproTech). The CAR expression on the surface of the NK-92 cells was evaluated by flow cytometry 48-72 h after transduction.

In vitro mRNA synthesis and mRNA electroporation

For CAR mRNA synthesis *in vitro,* the PD-L1-CAR construct was subcloned into pCIpA102 plasmid (a kind gift of Stein Sæbøe-Larssen from OUS). Linearized plasmid was cleaned up using QIAquick PCR Purification Kit (Qiagen) and was utilized as a template in mRNA synthesis reaction (Promega RiboMax Large Scale). ARCA (Anti Reverse Cap Analog) was used in the mRNA synthesis reaction to ensure proper cap orientation and by that 100% mRNA activity. Produced mRNA in concentration 1 µg/µl was stored at -80°C. Primary NK cells were magnetically isolated from PBMC using EasySep™ Human NK Cell Isolation Kit (StemCell Technologies) and activated for 3 days by adding 20 ng/ml IL-15. Then, the cells were electroporated with PD-L1-CAR mRNA. The procedure was performed using Gene Pulser Xcell Electroporation Systems (BioRad) in 0.4 cm Gene Pulser/Micropulser electroporation cuvettes (BioRad). 2×10^6 of NK cells suspended in 400 µl of Opti-MEM Reduced Serum Medium (ThermoFisher) were mixed with 20 or 40 µl (1 µg/µl) of previously synthesized mRNA or water (for MOCK control). After the electroporation (500 V, 2 ms, squarewave), cells were transferred onto a 6-well plate containing 2 ml of pre-warmed complete medium supplemented with 20 ng/ml of IL-15 for NK cells. After 18 h, the PD-L1-CAR expression was evaluated by flow cytometry.

CAR surface staining

To assess CAR surface expression, the effector cells (T, NK, or NK-92 cells) were washed 3 times with EasySep buffer (PBS supplemented with 2% FBS and 1 mM EDTA) and stained using goat anti-human IgG, Fcγ fragment specific antibody conjugated with Alexa Fluor 647 (Jackson ImmunoResearch Labs Cat# 109-606-098, RRID:AB_2337899, dilution 1:200) detecting a CH2-CH3 full hinge or CH3 half hinge region of the PD-L1-CAR or CD19-CAR. For cells modified with SFG CD19-CAR construct rituximab was

used at the concentration 10 µg/ml with consecutive anti-human IgG, Fcγ fragment specific antibody conjugated with Alexa Fluor 647. For HER2-CAR detection, the truncated version of human CD34 was detected by CD34 monoclonal antibody conjugated with APC (Thermo Fisher Scientific Cat# 17-0349-42, RRID:AB_2016672, dilution 1:50).

Generation target cell lines for luciferase based killing assays

HEK293T cells were modified with plasmid pLenti7.3/V5 TOPO-RedLuc encoding the red luciferase gene and green fluorescent protein, as described previously [5].

Generation of PD-L1- knockout and PD-L1-overexpressing target cell lines

Target cell lines unmodified or expressing luciferase reporter were used to generate cell models varying in PD-L1 expression. To obtain PD-L1 knockout of MDA-MB-231 cells, sgRNA sequences towards PD-L1 were selected from the Human CRISPR Knockout Pooled Library Brunello database (ACATGTCAGTTCATGTTCAG and ACTGCTTGTCCAGATGACTT) and cloned into the lentiviral vector pLentiCRISPv.2 plasmid, which was a gift from Feng Zhang (RRID:Addgene_52961 [6]). As a control, the construct with sgRNA towards a non-mammalian targeting control (NTC) was used. To generate MCF-7 and HEK-293T-PD-L1 overexpressing cells, the cDNA sequence of PD-L1 (NM_014143.2, Origene) was cloned into pLVX-IRES-PURO. MCF-7 and HEK-293T cells were modified with pLVX-IRES-PURO or pLVX-PD-L1-IRES-PURO constructs using lentiviral transduction. Two days after transduction, puromycin at 2 µg/ml was added to enforce the selection of the modified cells.

Induction of PD-L1 on the cell surface of effector cells

PD-L1 expression on unmodified T cells or CAR-modified T cells was monitored in time using flow cytometry. On day 0, T cells (or CAR-T cells directly after transduction) were cultured in the presence of 100 U/ml of IL-2 alone. After 24 h, the human T-activator CD3/CD28 beads were added, and cells were cultured for the next 6 days. To monitor PD-L1 surface expression in NK-92 cells upon antigen stimulation, parental, CD19-CAR NK-92, and PD-L1-CAR NK-92 cells were seeded onto a 12-well plate at density 1×10^6 mln per well in 1 ml full RPMI-1640 medium. Raji PD-L1 cells were added to the effector cells in a 1:1 effector:target ratio in a 2 ml full RPMI-1640 medium. After 24 h and 48 h co-culture, the cells were washed with PBS and stained with viability dye (Zombie NIR, cat. No., BioLegend, dilution 1:400), followed by CD56 (cat. No. 318328, Biolegend, clone HCD56, dilution 1:50) and PD-L1 staining (cat. No. 12-5983-42, eBioscience, clone MIH-1, dilution 1:100). The PD-L1 expression was analyzed by flow cytometry.

PD-L1 and HER-2 expression on target and effector cells

PD-L1 expression on target or effector cells was assessed using anti-PD-L1 antibody either clone MIH-1 antibody (Thermo Fisher Scientific Cat# 12-5983-42, RRID:AB_11042286, dilution 1:100) or clone 29E.2A3 (BioLegend Cat# 329734, RRID:AB_2629580, dilution 1:100). HER-2 expression on target cells was assessed using anti-HER2 antibody (BioLegend Cat# 324408, RRID:AB_2262301, dilution 1:100).

Functional assays (degranulation and cytokine release)

Degranulation of cytotoxic T cells and NK cells was performed by evaluating the expression of CD107a (LAMP-1) on the surface of T/NK cells with anti-CD107a antibody conjugated with fluorochrome. To this end, target cells were seeded at the round bottom 96-well plate in the presence of effector cells and CD107a-PE antibody (BD Biosciences Cat# 555801, RRID:AB_396135, dilution 1:40) and GolgiStop (BD Biosciences Cat# 554724, RRID:AB_2869012, dilution 1:250) and/or GolgiPlug (BD Biosciences Cat# 555029, RRID:AB_2869014, dilution 1:200). Typically, a 2:1 effector to target ratio was used for the functional assay. After 4 hours, cells were spun down, washed, and stained for the extracellular markers – CD3 for T cells (BD Biosciences Cat# 562426, RRID:AB_11152082, dilution 1:100), CD56 for NK, NK-92 cells (Miltenyi Biotec Cat# 130-113-308, RRID:AB_2726086, dilution 1:50) and Fixable Viability Dye to exclude dead cells (cat. No. L34963, Thermo Scientific, dilution 1:100). After fixation and permeabilization, intracellular staining for cytokines using anti-IFNγ (BD Biosciences Cat# 341117, RRID:AB_2264629, dilution 1:100) and anti-TNFα (BD Biosciences Cat# 557647, RRID:AB_396764, dilution 1:100) antibodies conjugated with fluorochromes was performed. Degranulation and cytokine production by effector cells was assessed using flow cytometry.

Flow cytometry-based killing assay

For fratricide cytotoxicity assay, target T cells were pre-stimulated for 24 h with human T-activator CD3/CD28 beads to induce PD-L1 expression on their surface. To separate target cells from effectors, target cells were stained with Cell Trace CFSE and effectors were stained with Cell Trace Violet (CTV). T cells were mixed and incubated with unmodified T cells, CD19-CAR or PD-L1 CAR T-cells for 24 h at E:T ratio 2:1. Propidium iodide (PI) was used to discriminate live/dead cells. Cytotoxicity of effector cells was evaluated as an increase in a percentage of green-CFSE (or violet-CTV) positive, PI positive target cell population

Preparation of T cells/NK-92 parental cells or PD-L1-CAR-T/NK-92 cell supernatants

MDA-MB-231 parental or sgPD-L1 breast cancer cells were seeded onto a 6-well plate at a cell density 1×10^6 mln per well in 2 ml full RPMI-1640 medium and left overnight to attach. Next, the medium was removed and replaced with either unmodified or PD-L1-CAR T or NK-92 parental or PD-L1-CAR NK-92 cells. The effector cells were added at a 1:1 E:T ratio and co-incubated for the next 24 h. Afterward,

the supernatants were collected, centrifuged at 2 000 × *g* for 5 min, and left for further experiments at -20°C.

Induction of PD-L1 on the cell surface of target cells

Cell lines were seeded onto the 24-well (or 12-well) plate at a cell density 1-2 × 10^5 per well. After 24 h, the medium was removed and changed either for the control (a fresh portion of RPMI-1640 full medium), or 25 ng/ml IFNγ, or conditioned supernatants from the 24-hour co-incubation cultures of unmodified T cells or PD-L1-CAR T cells with the target parental or sgPD-L1 MDA-MB-231 cells and incubated for the next 48 hours. Moreover, MCF-7 and SKBR-3 cells were co-incubated with HER-2-CAR T cells. For sequential killing experiments, MCF-7 cells were preincubated with or without 100 µg/ml trastuzumab for 24 h, and then incubated alone or together with T cells or HER-2 CAR T cells at an E:T ratio of 0.5:1. Then, the cells were detached with trypsin, washed with PBS, and stained with viability dye (Zombie NIR, cat. No. 423105, BioLegend, dilution 1:400 or Fixable Viability Stain 510, cat. No. 564406, BD Bioscience, dilution 1:20000) followed by PD-L1 staining (cat. No. 12-5983-42, eBioscience, clone MIH-1, dilution 1:100). The PD-L1 expression was analyzed by flow cytometry.

RTCA-based killing assay

For RTCA assay, adherent target cells were seeded onto 16-well E-Plates (ACEA Biosciences) at a cell density 3 × 10^4 per well in 100 µl of the appropriate medium and monitored in the incubator at 37°C (5% CO_2, 95% humidity) for 24 h with the xCELLigence impedance-based RTCA system (Acea Biosciences). Next, the medium was removed and replaced with RPMI-1640 full medium containing control or CAR-modified effector cells (primary T cells or NK92 cells) at various E:T ratios. For some experiments, 0.4 or 0.8 mg/ml atezolizumab (ATEZO, Roche) was added. The cells in the E-Plates were monitored with the RTCA system for the next 12-20 h. For the sequential killing, the first portion of CAR-T cells was added, and after 6-hour of impedance measurement, it was supplemented with the another portion of appropriate CAR-T cells and left for the next 16 h. Sequential killing experiments were performed in the presence or absence of 100 µg/ml of trastuzumab. The analysis of the results was performed using RTCA Software Pro (ACEA Biosciences). The impedance changes were normalized to the moment of the effector cells addition and plotted over time as normalized cell index.

Animals studies

The in vivo experiments were performed in the Animal Facility of the Medical University of Warsaw in accordance with the EU Directive 2010/63/EU and the Polish legislation for animal experiments of the Polish Ministry of Science and Higher Education (February 26, 2015) and approved by the Second Local Ethics Committee for the Animal Experimentation, Warsaw University of Life Sciences in Warsaw (for MDA-MB-231 study - WAW2/111/2019 and for MCF-7 - WAW2/108/2021). For the study, 6-12 old

female NSG (NOD.Cg-Prkdcscid Il2rgtm1Wjl/SzJ) mice (The Jackson Laboratory), were used. The experiments were carried out in SPF animal facility with IVC systems. To avoid confounders, all mice were labeled and kept in tagged cages. The cages had an assigned, unchanging place in the rack. Results obtained from individual mice or mesurement means according to the treatment method are presented. The blinding was not applied, however, the experiments were supervised by two experimenters, independently. The distribution of mice to the experimental groups was random and no animals were excluded during the experiment. The sample size was determined based on the assumed increase in tumor diameter. The experimental group size was calculated by power analysis or resource equation approach as described in [7].

In vivo treatments

MDA-MB-231 cells (1×10^6) were inoculated into the second, left mammary fat pad of NSG mice in 50% Matrigel (BD, USA), on day 0 of the experiment. Subsequently, on days 8 and 15, 5×10^6 PD-L1-CAR-T, CD19-CAR-T, or unmodified T cells were administrated intratumorally. Control mice were injected with PBS. Tumor growth was monitored two times per week with calipers and the tumor volume was calculated using the formula: volume = (length × width2)/2. The mice were sacrificed when the tumors reached 12 mm in diameter. Total number of mice used within this study – 38.

In the case of the experiments involving MCF-7 cells the slow-release pellets containing 17β-estradiol (Innovative Research of America, USA), were implanted subcutaneously four days before tumor cells inoculation. Then NSG mice were injected with 3×10^6 MCF-7 pLVX or MCF-7 PD-L1 cells into the second, left mammary fat pads in 50% Matrigel (BD, USA). Finally, the 5×10^6 PD-L1-CAR-T or control T cells or PBS were injected intratumorally on 24, 27, and 30 day of the experiment. Tumors were measured with calipers once per week. Total number of mice used within this study – 35.

Luciferase-based killing assays

HEK-293T cell lines (HEK-293T pLVX (PD-L1 $^{low/null}$) and HEK-293T PD-L1 (PD-L1^{positive})), previously modified to express luciferase reporter gene (Red-Luc), were seeded onto the 96-well black plates with a clear bottom (Perkin Elmer) at a cell density 2.5×10^4 per well in 100 µl of full DMEM medium in triplicates and allowed to adhere for 24 h. The next day, 100 µl of the medium was removed and replaced with 100 µl of culture medium with suspended effector cells. The cells were co-incubated at various effector to target ratios for 18 h at 37°C (5% CO_2, 95% humidity). Bright-Glo™ Luciferase Assay System (cat. No. E2610, Promega) was used for bioluminescence readout. 100 µl of the reagent was added to each well with the co-cultured cells. The plate was incubated for 5 min in darkness at 25°C, and then the luminescence was measured using Victor Plate Reader (Perkin Elmer).

Live imaging experiments (BM-MSC killing)

BM-MSCs were seeded onto the 96-well black plates with clear bottom (PerkinElmer) at a cell density 5×10^3 per well in 100 µl of DMEM medium supplemented with 10% FBS and 1% Pen/Strep in duplicates and allowed to adhere for 24 h. For the next 24 h, the cells were cultured in the presence or absence of 25 ng/ml of IFNγ. Afterward, to reduce background fluorescence, the medium was replaced with FluoroBrite DMEM (Life Technologies) medium supplemented with 10% FBS, 1% Pen/Strep, and 2 mM L-glutamine, and the effector NK-92 parental or PD-L1-CAR-modified cells were added at the E:T ratio of 0.5:1 for 8 h. To assess apoptosis progression, the 0.5 µM of CellEvent Caspase-3/7 Green Detection Reagent (cat. No. C10427, Thermo Scientific) was added. The apoptosis of the BM-MSCs in the presence of NK-92 cells was monitored in real-time using Cytation™ 1 Cell Imaging Multi-Mode Reader with 15 min intervals. Consecutive images were acquired at defined time points for 8 h using 488-nm excitation and collecting fluorescence emission using a 530/30 bandpass filter. The number of Caspase-3/7 positive cells was calculated using Gene 5 3.04 software (BioTek, Agilent).

Cytokine array

The cytokine arrays were co-incubated with the supernatants collected from the 24-h co-cultures of MDA-MB-231 parental breast cancer cells with T cells/NK-92 parental (control) or PD-L1-CAR T/NK-92 cells overnight at 4°C with shacking. The array procedure was performed using R&D Systems Human Cytokine Array, Panel A (cat. No. ARY005, R&D Systems) according to the manufacturer's protocol. The signals on the developed membrane were visualized by chemiluminescence detection using ChemiDoc Imaging System (Bio-Rad Laboratories, Hercules, CA, USA). The densitometric analysis was performed using Image Lab software (Bio-Rad Laboratories, RRID:SCR_014210, Hercules, CA, USA) and GraphPad Prism 8 (GraphPad Software, RRID:SCR_002798, San Diego, CA, USA).

Statistical analysis

Statistical analysis was performed with GraphPad Prism 8 (GraphPad Prism, RRID:SCR_002798). Results are shown as the mean value ± standard deviation (SD) unless otherwise stated. Normality was checked using the Shapiro-Wilk test. The comparison between two groups for paired samples was analyzed using Student t-test or Wilcoxon test and for unpaired samples using unpaired t-test or Mann-Whitney test depending on data distribution. For the in vivo experiment, a two-way ANOVA test was applied. The P values of less than 0.05 were considered significant.

Supplementary Figure Legends

Suppl. Figure 1. Expression of PD-L1 in cancer cell lines.

A. *The representative Western Blot analysis of PD-L1 expression (PD-L1 antibody, clone E1L3N, cat. No. 13684, Cell Signaling, dilution 1:1000) in ovarian (A2774, A2780, OvaCa3, MDAH), cervical (HeLa), Hodgkin lymphoma (L540, L428, SUP-HD1, HDLM-2), non-small cell lung cancer (A549) and melanoma (M407, M257) cancer cell lines. The experiment was repeated three times.*

B. *Representative density plots and histogram overlays illustrating PD-L1 expression (red) against a background from isotype control (grey) for the HCC1806 breast cancer cell line using flow cytometry. The staining was performed using an anti-PD-L1 antibody (cat. no. 12-5983-42, eBioscience, clone MIH1, dilution 1:100). Numbers on the density plots indicate the percentage (%) of PD-L1 positive cells. The experiment was repeated at least two times.*

C. *Representative density plots and histogram overlays illustrating PD-L1 expression (red) against a background from isotype control (grey) for MCF-7 (upper panel) and MDA-MB-231 (lower panel) breast cancer cell lines using flow cytometry. The staining was performed using an anti-PD-L1 antibody (cat. No. 329734, BioLegend, clone 29E.2A3, dilution 1:100). Numbers on the density plots indicate the percentage (%) of PD-L1 positive cells. The experiment was repeated at least three times.*

Suppl. Figure 2. Time-dependent enrichment in PD-L1-CAR-T presence in the population of the transduced T cells, transient NK cells modifications using mRNA electroporation technique and selection of PD-L1-CAR NK-92 positive population by FASC sorting.

A. *Flow cytometry analysis of the surface PD-L1-CAR expression was assessed 3 and 10 days following the lentiviral transduction with PD-L1-CAR encoding vector. Unmodified and PD-L1-CAR T cells were washed with EasySep buffer (PBS supplemented with 2% FBS and 1 mM EDTA) and stained using goat anti-human IgG, Fcγ fragment specific antibody conjugated with Alexa Fluor 647 (cat. No. 109-606-098, Jackson ImmunoResearch) diluted 1:200 in EasySep buffer.*

B. *Flow cytometry analysis of the surface PD-L1-CAR expression in NK cells after mRNA electroporation form two experiments with three and two individual donors (n = 5, bar graph, left side) and representative flow cytometry density plots of PD-L1-CAR expression on the surface of mock (unmodified) and PD-L1-CAR-NK cells detected by anti-human IgG, Fcγ fragment specific antibody (right side). Numbers on the density plots indicate the percentage (%) of PD-L1-CAR positive cells.*

C. *PD-L1-CAR positive NK-92 cells were stained with anti-human IgG antibody recognizing Fcγ fragment and sorted based on their PD-L1-CAR expression using fluorescence-activated cell sorting (FACS) flow cytometry. Numbers on the density plots indicate the percentage (%) of PD-L1-CAR positive cells.*

Suppl. Figure 3. The expression pattern of PD-L1 after CAR T cells stimulation

A. *The scheme depicting the modular structure of CD19 CARs used within this study (for details see Materials and Methods Section).*

B. *PD-L1 expression on PD-L1- and CD19-CAR T cells stimulated by human T-activator CD3/CD28 beads and IL-2 (100 U/ml). CAR T cells were cultivated in the presence of 100 U/ml of IL-2 alone (Day 0)*

or together with human T-activator CD3/CD28 beads (Day 1-6). Day 1 represents the first day after the stimulation of T cells with human T-activator CD3/CD28 beads. PD-L1 staining was performed on consecutive days using an anti-PD-L1 (clone MIH1, dilution 1:100). The experiment was repeated in duplicate two times.

- ***C.*** *Flow cytometry analysis of fratricide killing performed by PD-L1-CAR T cells. The left-hand panel depicts the scheme and timeline of the experiment. The right-hand panel presents the killing potential of effectors (CTV stained PD-L1-CAR-T or CD19-CAR T cells) against unmodified T cells derived from the same donor and stimulated with human T-activator CD3/CD28 beads and IL-2 (100 U/ml) for 24 h and stained with CFSE prior to the experiment. Effector cells (PD-L1-CAR-T cells or CD19-CAR-T cells) were added to the targets - unmodified T cells at the E:T ratio of 2:1 in the absence or presence of 0.6 mg/ml atezolizumab. After 24 h propidium iodide was added and the percentage (%) of the CFSE and PI positive cells was assessed with flow cytometry. The experiment was repeated in duplicates two times.*
- ***D.*** *The representative Western Blot analysis of PD-L1 expression (PD-L1 antibody, clone E1L3N, cat. No. 13684, Cell Signaling, dilution 1:1000) in PD-L1- and CD19-CAR T cells stimulated by human T-activator CD3/CD28 beads and IL-2 (100 U/ml). The lysates were collected collected in day 0 as well as in days 1, 4, and 7 post stimulation and day 8 after beads re-stimulation. The experiment was repeated two times. Bands were quantified by densitometry; the signal for the PD-L1 band was normalized to the corresponding actin band (lower panel).*
- ***E.*** *qPCR analysis of PD-L1 mRNA expression in unmodified T cells, PD-L1- and CD19-CAR T cells stimulated by human T-activator CD3/CD28 beads and IL-2 (100 U/ml). mRNA was collected on day 0 as well as in days 1, 4, and 7 post-stimulation and day 8 after beads re-stimulation. The experiment was repeated in duplicate two times.*
- ***F.*** *Phenotypic characteristics of PD-L1-CAR T cells. The differentiation and exhaustion markers on the surface of unmodified T cells, CD19-CAR T, and PD-L1-CAR T cells were performed on days 4 and 10 after CARs transduction and analyzed by flow cytometry.*

Suppl. Figure 4. The efficacy of PD-L1-CAR NK-92 and primary NK cells against breast cancer cells and generation of the PD-L1-knockout derivative of MDA-MB-231 cell line and the PD-L1-overexpressing derivative of MCF-7 cell line and their susceptibility to PD-L1-CAR NK-92 cells cytotoxic activity.

- ***A.*** *Functional and cytokine release assays of PD-L1-CAR NK-92 cells targeted against MCF-7 (PD-L1$^{low/-}$) or MDA-MB-231 (PD-L1^{+}) cancer cell lines were assessed by flow cytometry. Degranulation assay, assessed by CD107a staining (left panel), and IFNγ release (right panel) were measured after 5 h of co-incubation of target and effector cells at the E:T ratio of 2:1. The experiment was repeated in duplicates. Bars represent the ± SD with the p-values derived from unpaired t-test (*p < 0.05, **p < 0.01).*
- ***B.*** *Degranulation (measured by CD107a, left panel) and IFNγ release (right panel) assays of PD-L1-CAR NK cells targeted against MDA-MB-231 (PD-L1^{+}) cancer cell line were assessed by flow cytometry. The experiment was performed two times, with three and two individual donors (n = 5). Bars represent the mean value ± SD. The differences between groups were analyzed using unpaired t-test (*p < 0.05, ***p < 0.001).*
- ***C.*** *Representative flow cytometry density plots showing efficient ablation of PD-L1 by CRISPR/Cas9 in MDA-MB-231 cells. PD-L1 surface presence was assessed using anti-PD-L1 antibody (clone 29E.2A3).*

D. *Western blot analysis of PD-L1 expression in unmodified (parental) and two knockouts (KO clone 1 and 2) MDA-MB-231 cells. β-actin was used as a loading control. The experiment was repeated three times.*

E. *Representative flow cytometry histograms showing overexpression of PD-L1 by lentiviral transduction of MCF-7 cells (MCF-7 PD-L1) compared to empty vector-modified MCF-7 cells (MCF-7 pLVX). PD-L1 surface presence was assessed using anti-PD-L1 antibody (clone 29E.2A3).*

F. *Western blot analysis of PD-L1 expression in control (parental, pLVX) and PD-L1 overexpressing MCF-7 cells. β-actin was used as a loading control. The experiment was repeated three times.*

G. *Degranulation and IFNγ release assays of PD-L1-CAR NK-92 cells targeted against MCF-7 pLVX (PD-L1$^{low/-}$) and MCF-7 PD-L1 or MDA-MB-231 sgNTC (PD-L1^{+}) or MDA-MB-231 sgPD-L1 (PD-L1^{-}) cancer cell lines were assessed by flow cytometry. Degranulation assay assessed by CD107a (left panel) staining and IFNγ release (right panel) were measured after 2.5 h of co-incubation of target and effector cells at the E:T ratio of 2:1. The experiment was repeated in duplicates. Bars represent the mean value ± SD. The differences between control and CAR-affected groups were analyzed using unpaired t-test (*p < 0.05, **p < 0.01, ***p < 0.001).*

H. *The cytotoxic activity of PD-L1-CAR-T cells against T47D cell line, at the E:T ratio of 1:1 and 2:1 were measured by impedance analysis. Samples were internally normalized for the cell index value measured before CAR-T cells addition (Normalized Cell Index plots). Representative average impedance curves from 2 wells are shown. The experiment was repeated in duplicates two times.*

I. *The growth of MDA-MB-231 tumors injected with PBS (control) vs tumors injected with T cells, CD19- or PD-L1-CAR T cells in mice (initial n=8 mice/group). A single tumor volume plots vs. the number of days post first CAR injection are depicted.*

J. *The growth of MCF7-pLVX tumors injected with PBS (control) vs. tumors injected with T cells or PD-L1-CAR T cells in mice (initial n=6-7 mice/group), left panel. The growth of MCF7-PD-L1 tumors injected with PBS (control) vs. tumors injected with T cells or PD-L1-CAR T cells in mice (initial n=4-7 mice/group), right panel.*

Suppl. Figure 5. Induction of PD-L1 expression on the target cells after different stimuli.

A. *PD-L1 expression induced on cancer cells by supernatant from activated CAR T cells was assessed by flow cytometry. The control (only medium) and conditioned supernatants from the 24-hour co-cultures of control (unmodified) or PD-L1-CAR T cells with the target MDA-MB-231 cells were transferred onto the culture of sgNTC and sgPD-L1 MDA-MB-231 and incubated for 24 hours. Next, PD-L1 surface presence was assessed by flow cytometry using anti-PD-L1 antibody (clone MIH1). The experiment was repeated two times.*

B. *IFNγ induced expression of PD-L1 on breast cancer cells (MDA-MB-231 and MCF-7) was assessed by flow cytometry. PD-L1 staining was performed using anti-PD-L1 antibody (clone MIH1).*

C. *Representative images of different subpopulations of macrophages (M0, M0+IFNγ, M2) stained for PD-L1 assessed by immunocytochemistry assay using Cytation 1 Cell Imaging Multi-Mode Reader (Biotek, Agilent). The control (only medium) and conditioned supernatants from the 24-hour cultures of MDA-MB-231, MDA-MB-231 sgPD-L1, or MDA-MB-231 cells co-incubated with CAR PD-L1 T cells were transferred onto different subpopulations of macrophages and incubated for 48 hours. Next, PD-L1 surface presence was assessed using the anti-PD-L1 antibody (clone MIH1). The signal was developed using AF488-conjugated secondary antibody (green), and nuclei were counterstained with DAPI (blue), scale bar: 100 µm. The background fluorescence was removed*

and the low threshold for green fluorescence was set to create a mask of the area covered by macrophages. Bar graphs represent the mean fluorescent intensity of PD-L1 within the thresholded area. The experiment was performed in duplicates with two donors (n = 2).

D. *The representative Western blot results of cytokine array assay performed with the supernatants collected from control unmodified T or PD-L1-CAR T (left hand panels) and NK-92 or PD-L1-CAR NK-92 cells (right-hand panels) co-cultured with MDA-MB-231 breast cancer cells for 24 h at 1:1 E:T.*

Suppl. Figure 6. The efficacy of HER-2-CAR T cells against MCF-7 breast cancer cells.

A. *The scheme depicting the modular structure of HER-2-CAR.*

B. *Flow cytometry analysis of HER-2-CAR expression in control (upper panels) and lentiviral transduced T cells (lower panels). HER-2-CAR expression was detected using anti-human CD34 antibody (cat. No. 17-0349-42, eBioscience™). Numbers on the density plots indicate the percentage (%) of HER-2-CAR positive cells. The experiments were repeated at least three times.*

C. *The potential of killing tumor cells by HER-2-CAR-T cells was measured by impedance analysis for MCF-7 cells. Cells were left to adhere and to form a monolayer on the E-plates for 24 h. The next day, HER-2-CAR-T cells were added to the monolayers for 12 hours at the indicated E:T ratios. Representative impedance curves were shown. The experiment was repeated in duplicate two times.*

D. *HER-2 surface expression on MCF-7 and SKBR-3 (as positive control) cells was assessed by flow cytometry with an anti-HER-2 antibody (Cat. No. 324408, BioLegend). Bar graph showing the average mean fluorescent intensity of PD-L1 expression in MCF-7 and SKBR-3 cells compared to the isotype control. Bar graph represents the average MFI from two experiments performed in duplicates.*

Suppl. Figure 7. The killing potential of CAR-PD-L1-bearing NK-92 cells towards the bone marrow-derived mesenchymal stem cells and generation of the PD-L1 overexpressing HEK-293T cell line.

A. *BM-MSC cells were cultured in the presence or absence of 25 ng/ml of IFNγ for 24 h. Next, the effector NK-92 parental or CAR PD-L1 cells were added at the E:T ratio of 0.5:1 for 8 hrs. To assess apoptosis progression, the CellEvent Caspase-3/7 Green Detection Reagent was added. Apoptosis of the BM-MSC cells was monitored in real-time using Cytation™ 1 Cell Imaging Multi-Mode Reader in 15 min intervals. The number of Caspase-3/7 positive cells was calculated using Gene 5 3.04 software (BioTek, Agilent). The experiment was repeated in duplicate for six individual BM-MSC donors. Statistical analysis was performed within a time-point. Normality was checked using the Shapiro-Wilk test. The p-values derived from the Student t-test are presented for BM-MSC + IFNγ + CAR-PD-L1 NK-92 (dark red line) comparing to BM-MSC + CAR-PD-L1 NK-92 (red line) samples (*p < 0.05; **p < 0.01). Representative images were showing the detection of apoptosis of BM-MSC (preincubated with or without 10 ng/ml IFNγ) upon incubation with CAR PD-L1-bearing NK-92 cells using CellEvent Caspase-3/7 Green Detection Reagent in selected time points (0, 2, 4, 6, 8 h).*

B. *The generation of the PD-L1 overexpressing derivative of HEK-293T Red-Luc cell line (containing stably transduced Red-Luc luciferase) by lentiviral transduction. Representative flow cytometry histograms showing surface overexpression of PD-L1 on HEK-293T Red-Luc (HEK-293T-PD-L1) compared to control (HEK-293T-pLVX, transduced with empty vector). The PD-L1 surface expression was assessed using anti-PD-L1 antibody (clone MIH1).*

1 Demaison C, Parsley K, Brouns G, Scherr M, Battmer K, Kinnon C *et al*. High-level transduction and gene expression in hematopoietic repopulating cells using a human immunodeficiency [correction of imunodeficiency] virus type 1-based lentiviral vector containing an internal spleen focus forming virus promoter. *Hum Gene Ther* 2002; 13: 803-813.

2 Priceman SJ, Tilakawardane D, Jeang B, Aguilar B, Murad JP, Park AK *et al*. Regional Delivery of Chimeric Antigen Receptor-Engineered T Cells Effectively Targets HER2(+) Breast Cancer Metastasis to the Brain. *Clin Cancer Res* 2018; 24: 95-105.

3 Köksal H, Baken E, Warren DJ, Løset GÅ, Inderberg EM, Wälchli S. Chimeric antigen receptor preparation from hybridoma to T-cell expression. *Antibody Therapeutics* 2019; 2: 56-63.

4 Soneoka Y, Cannon PM, Ramsdale EE, Griffiths JC, Romano G, Kingsman SM *et al*. A transient three-plasmid expression system for the production of high titer retroviral vectors. *Nucleic Acids Res* 1995; 23: 628-633.

5 Bajor M, Zych AO, Graczyk-Jarzynka A, Muchowicz A, Firczuk M, Trzeciak L *et al*. Targeting peroxiredoxin 1 impairs growth of breast cancer cells and potently sensitises these cells to prooxidant agents. *Br J Cancer* 2018; 119: 873-884.

6 Sanjana NE, Shalem O, Zhang F. Improved vectors and genome-wide libraries for CRISPR screening. *Nat Methods* 2014; 11: 783-784.

7 Charan J and Kantharia ND. How to calculate sample size in animal studies? J Pharmacol Pharmacother. 2013 Oct;4(4):303-6

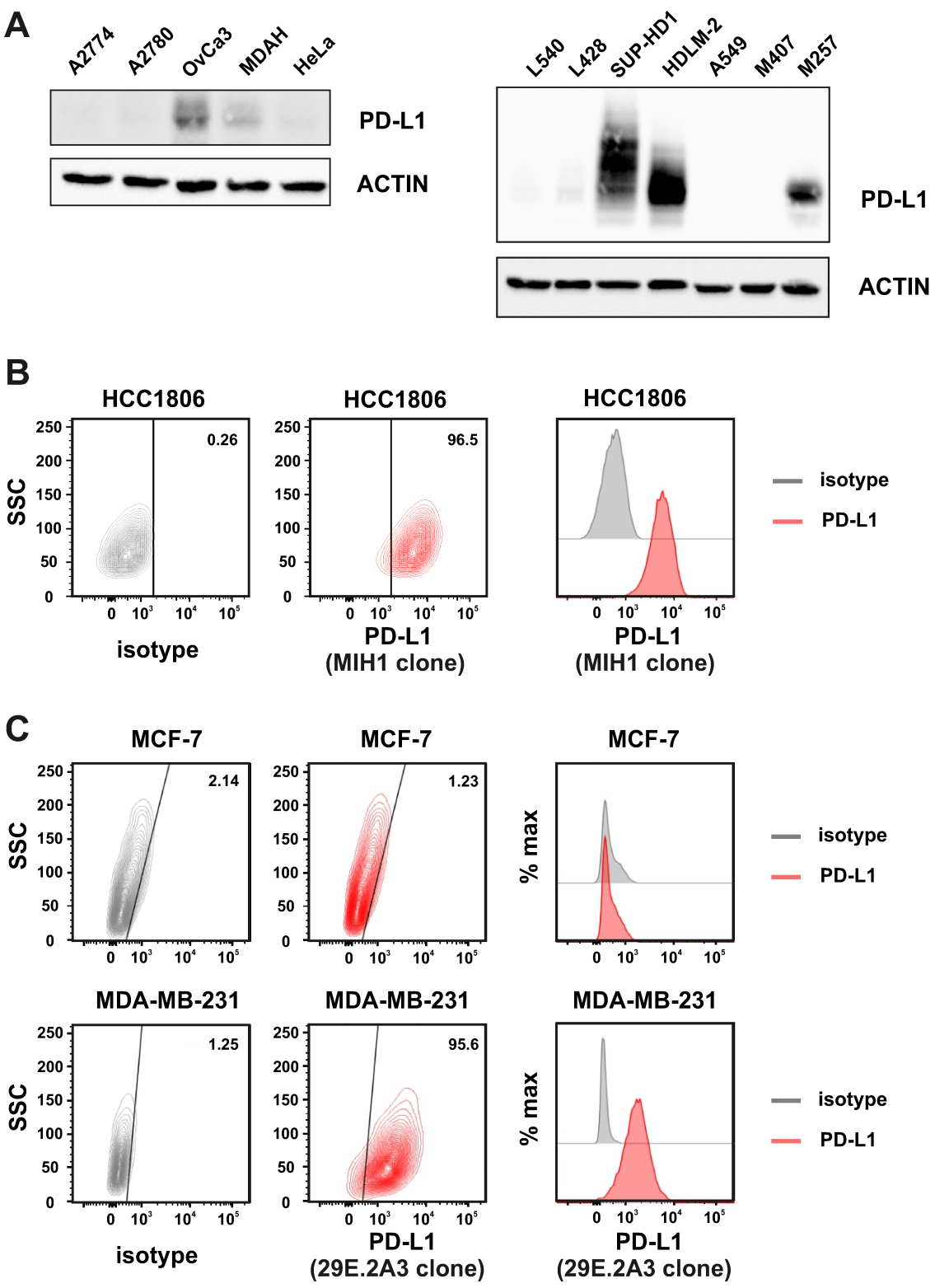
A
A2774
A2780
OvCa3
MDAH
HeLa
PD-L1
ACTIN
L540
L428
SUP-HD1
HDLM-2
A549
M407
M257
PD-L1
ACTIN
B
HCC1806
HCC1806
HCC1806
SSC
0.26
96.5
isotype
PD-L1
(MIH1 clone)
PD-L1
(MIH1 clone)
isotype
PD-L1
C
MCF-7
MCF-7
MCF-7
SSC
2.14
1.23
% max
MDA-MB-231
MDA-MB-231
MDA-MB-231
isotype
PD-L1
1.25
95.6
isotype
PD-L1
(29E.2A3 clone)
PD-L1
(29E.2A3 clone)

Suppl Fig.1

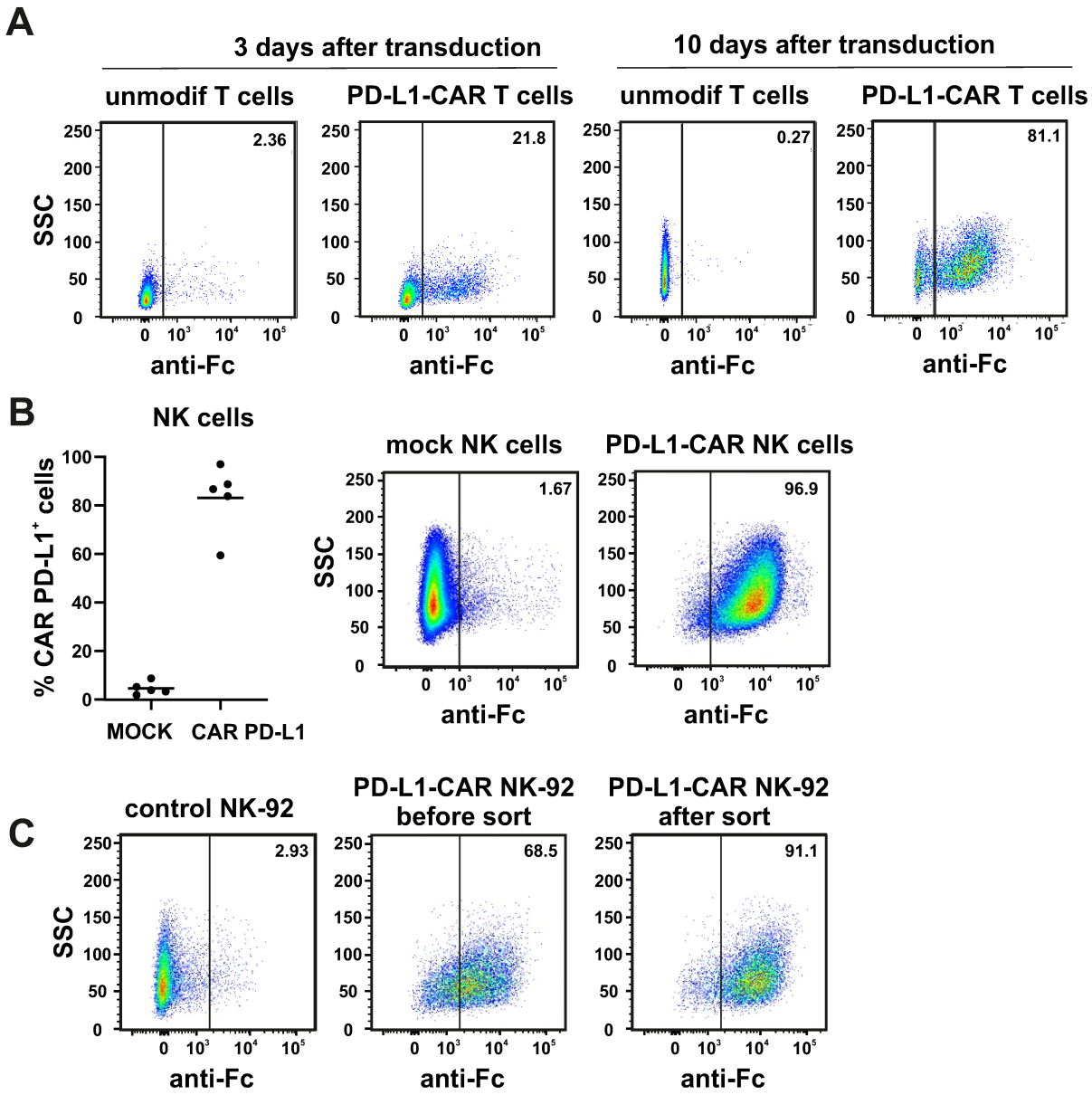
A
3 days after transduction
10 days after transduction
unmodif T cells
PD-L1-CAR T cells
unmodif T cells
PD-L1-CAR T cells
2.36
21.8
0.27
81.1
SSC
anti-Fc
B
NK cells
% CAR PD-L1+ cells
MOCK
CAR PD-L1
mock NK cells
PD-L1-CAR NK cells
1.67
96.9
C
control NK-92
PD-L1-CAR NK-92 before sort
PD-L1-CAR NK-92 after sort
2.93
68.5
91.1

Suppl Fig.2


A
anti-CD19 scFv
CD8 TM
4-1BB
CD3ζ
anti-CD19 scFv
IgG1 hinge
CD28
TM
CD3ζ

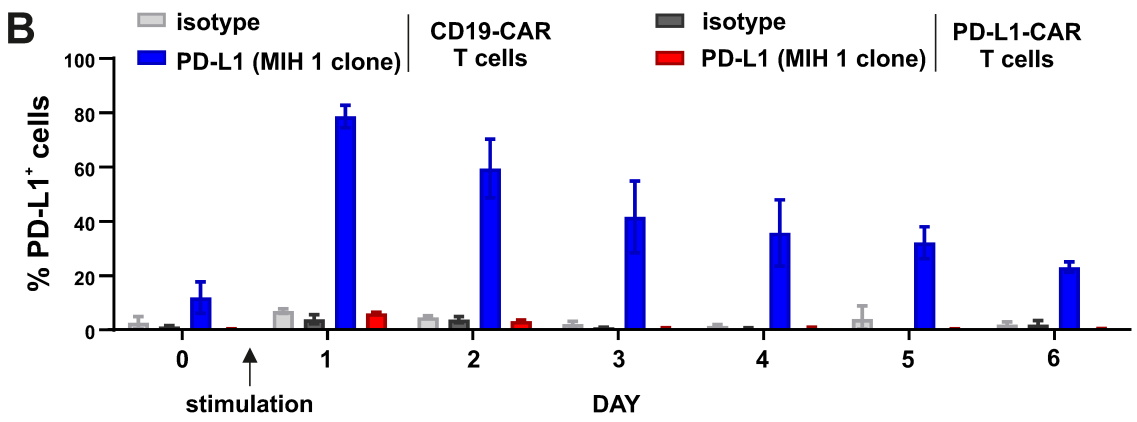
B
isotype
PD-L1 (MIH 1 clone)
CD19-CAR T cells
isotype
PD-L1 (MIH 1 clone)
PD-L1-CAR T cells
% PD-L1+ cells
stimulation
DAY

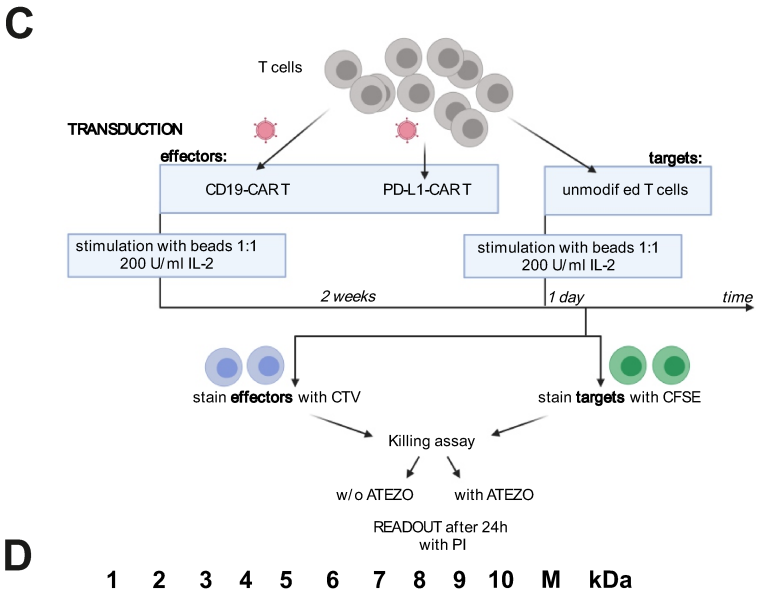
C
T cells
TRANSDUCTION
effectors:
CD19-CAR T
PD-L1-CAR T
targets:
unmodif ed T cells
stimulation with beads 1:1
200 U/ml IL-2
stimulation with beads 1:1
200 U/ml IL-2
2 weeks
1 day
time
stain effectors with CTV
stain targets with CFSE
Killing assay
w/o ATEZO
with ATEZO
READOUT after 24h
with PI

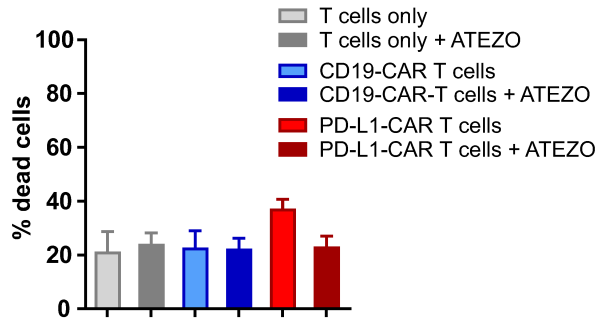
T cells only
T cells only + ATEZO
CD19-CAR T cells
CD19-CAR-T cells + ATEZO
PD-L1-CAR T cells
PD-L1-CAR T cells + ATEZO
% dead cells

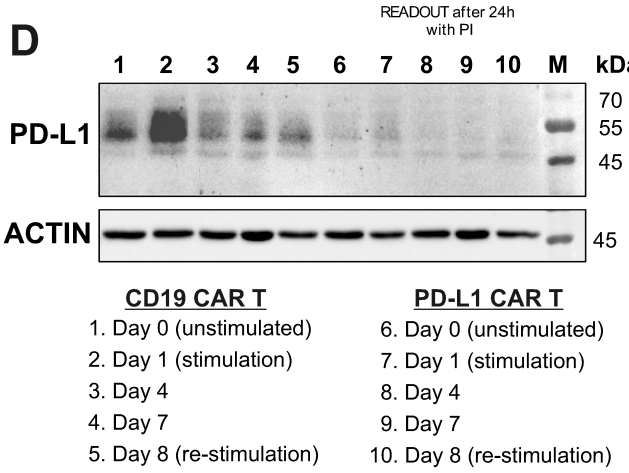
D
1 2 3 4 5 6 7 8 9 10 M kDa
PD-L1
70
55
45
ACTIN
45
CD19 CAR T
1. Day 0 (unstimulated)
2. Day 1 (stimulation)
3. Day 4
4. Day 7
5. Day 8 (re-stimulation)
PD-L1 CAR T
6. Day 0 (unstimulated)
7. Day 1 (stimulation)
8. Day 4
9. Day 7
10. Day 8 (re-stimulation)

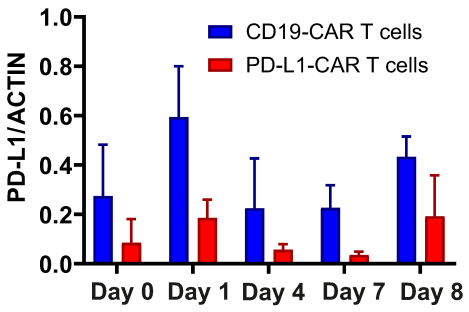
PD-L1/ACTIN
CD19-CAR T cells
PD-L1-CAR T cells
Day 0 Day 1 Day 4 Day 7 Day 8

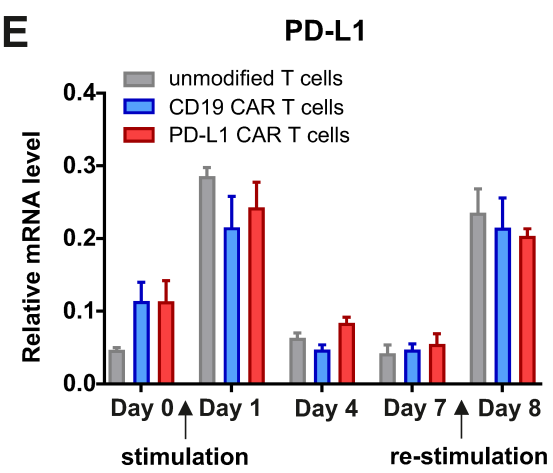
E
PD-L1
unmodified T cells
CD19 CAR T cells
PD-L1 CAR T cells
Relative mRNA level
Day 0 Day 1 Day 4 Day 7 Day 8
stimulation
re-stimulation

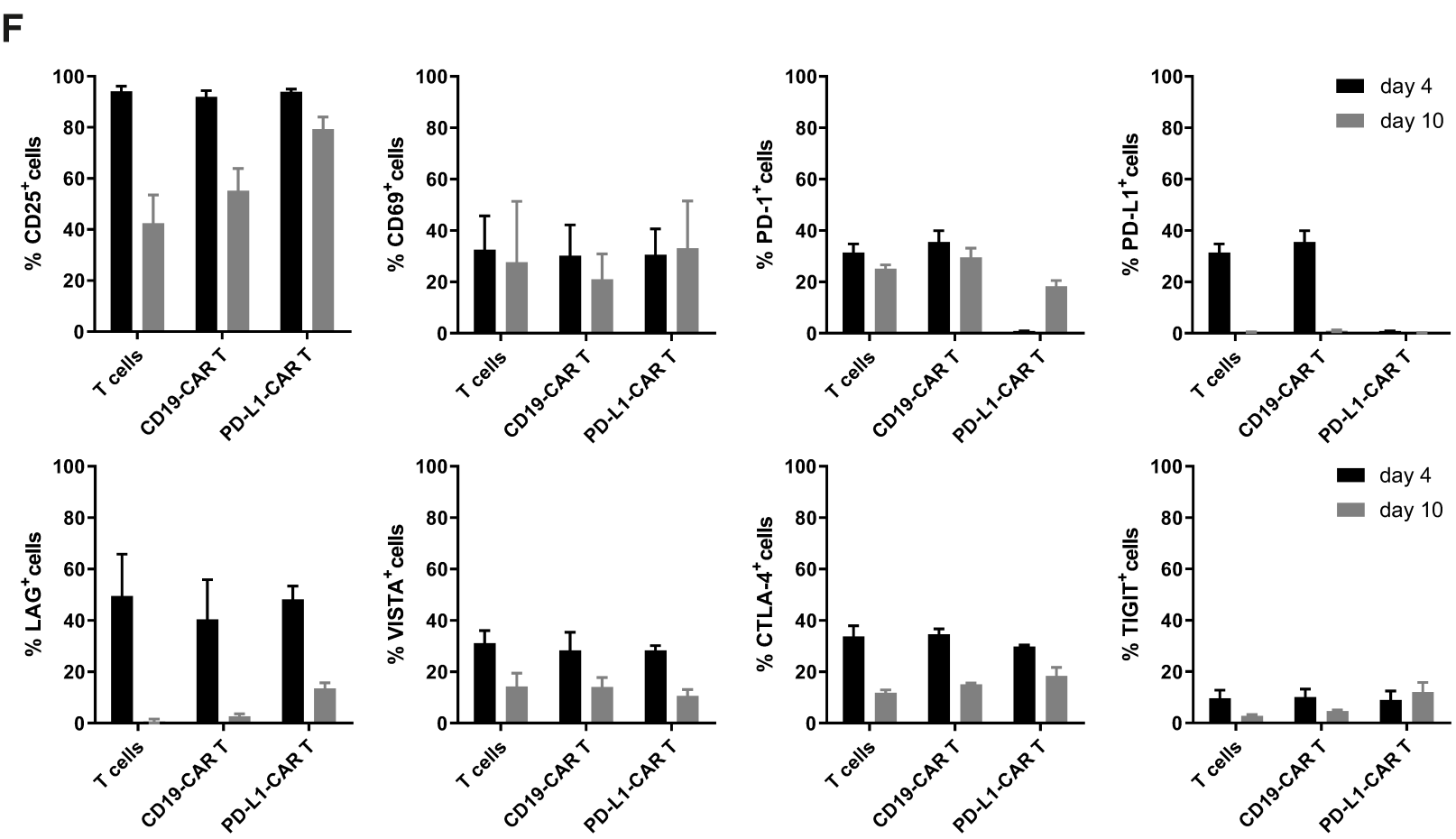
F
% CD25+ cells
% CD69+ cells
% PD-1+ cells
% PD-L1+ cells
% LAG+ cells
% VISTA+ cells
% CTLA-4+ cells
% TIGIT+ cells
day 4
day 10
T cells
CD19-CAR T
PD-L1-CAR T

Suppl Fig.3

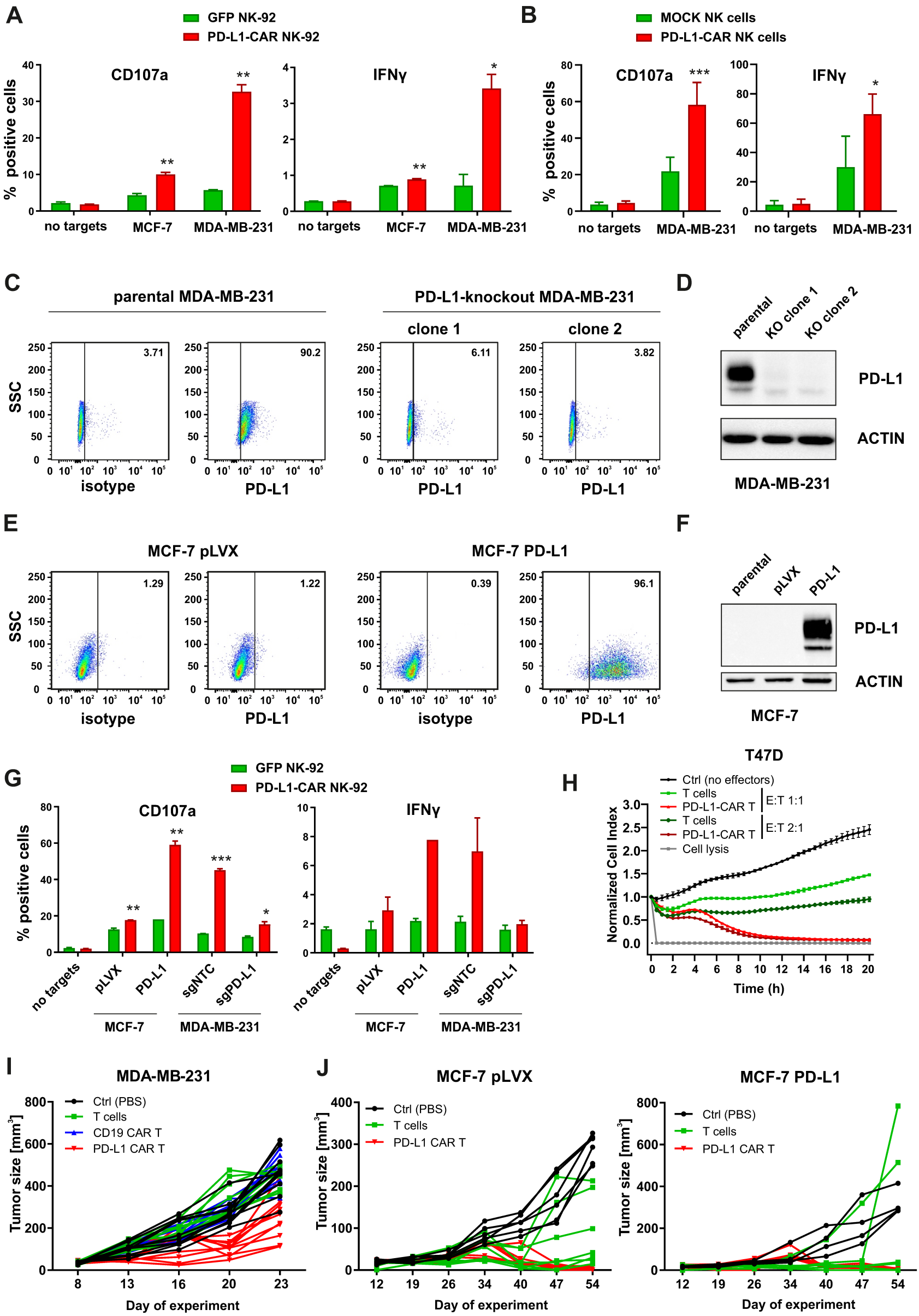
A
GFP NK-92
PD-L1-CAR NK-92
CD107a
IFNγ
% positive cells
no targets
MCF-7
MDA-MB-231
B
MOCK NK cells
PD-L1-CAR NK cells
C
parental MDA-MB-231
PD-L1-knockout MDA-MB-231
clone 1
clone 2
SSC
isotype
PD-L1
3.71
90.2
6.11
3.82
D
parental
KO clone 1
KO clone 2
PD-L1
ACTIN
MDA-MB-231
E
MCF-7 pLVX
MCF-7 PD-L1
1.29
1.22
0.39
96.1
F
pLVX
MCF-7
G
sgNTC
sgPD-L1
H
T47D
Ctrl (no effectors)
T cells
PD-L1-CAR T
Cell lysis
E:T 1:1
E:T 2:1
Normalized Cell Index
Time (h)
I
MDA-MB-231
Ctrl (PBS)
CD19 CAR T
PD-L1 CAR T
Tumor size [mm³]
Day of experiment
J
MCF-7 pLVX
MCF-7 PD-L1

Suppl Fig.4

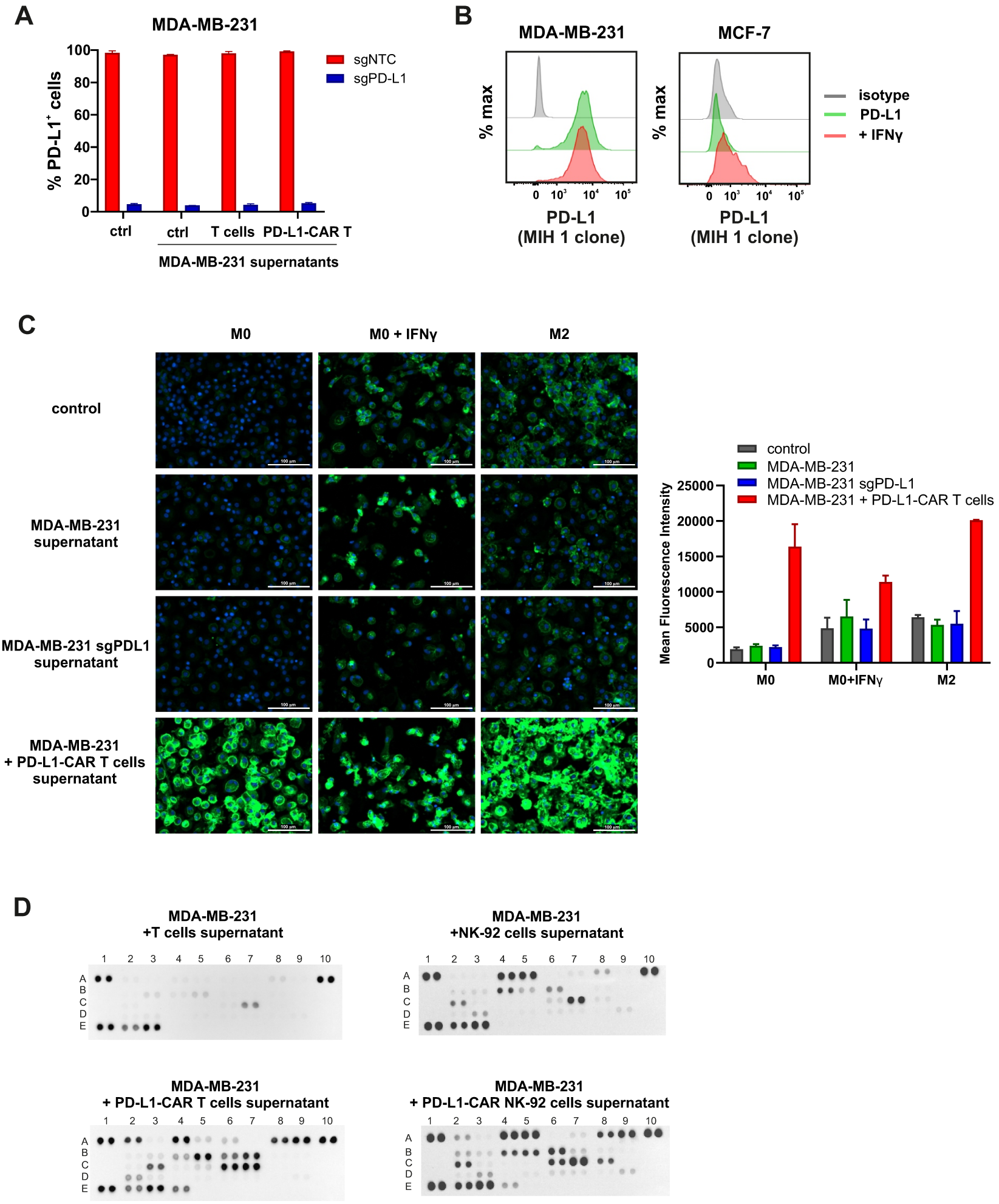
A
MDA-MB-231
% PD-L1+ cells
100
80
60
40
20
0
sgNTC
sgPD-L1
ctrl
ctrl
T cells
PD-L1-CAR T
MDA-MB-231 supernatants
B
MDA-MB-231
MCF-7
% max
% max
0
10^3
10^4
10^5
PD-L1
(MIH 1 clone)
PD-L1
(MIH 1 clone)
isotype
PD-L1
+ IFNγ
C
M0
M0 + IFNγ
M2
control
MDA-MB-231 supernatant
MDA-MB-231 sgPDL1 supernatant
MDA-MB-231 + PD-L1-CAR T cells supernatant
100 µm
control
MDA-MB-231
MDA-MB-231 sgPD-L1
MDA-MB-231 + PD-L1-CAR T cells
Mean Fluorescence Intensity
25000
20000
15000
10000
5000
0
M0
M0+IFNγ
M2
D
MDA-MB-231
+T cells supernatant
MDA-MB-231
+NK-92 cells supernatant
MDA-MB-231
+ PD-L1-CAR T cells supernatant
MDA-MB-231
+ PD-L1-CAR NK-92 cells supernatant
1 2 3 4 5 6 7 8 9 10
A
B
C
D
E

Suppl Fig.5

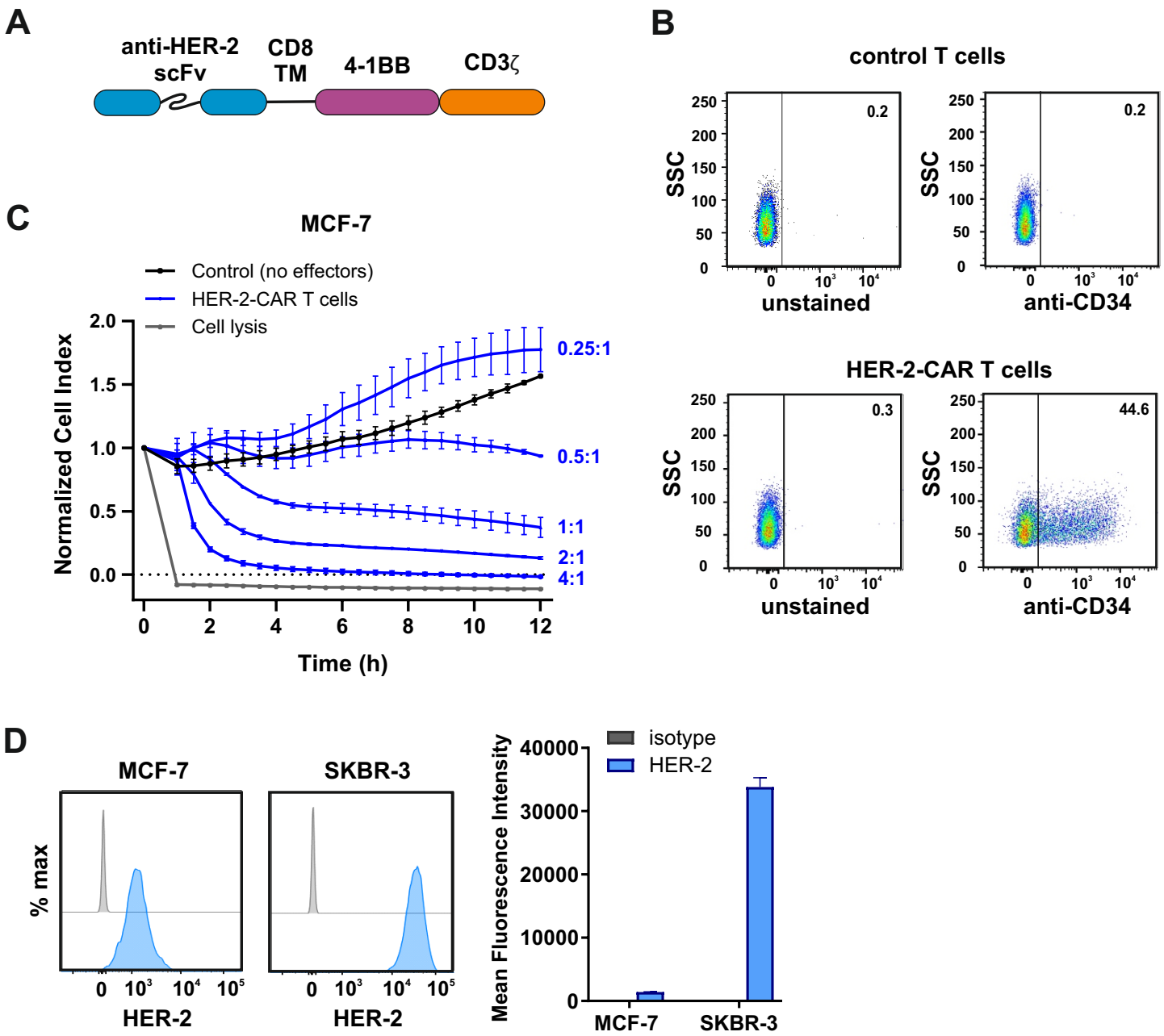
A
anti-HER-2 scFv
CD8 TM
4-1BB
CD3ζ
B
control T cells
SSC
unstained
anti-CD34
0.2
HER-2-CAR T cells
0.3
44.6
C
MCF-7
Control (no effectors)
HER-2-CAR T cells
Cell lysis
Normalized Cell Index
Time (h)
0.25:1
0.5:1
1:1
2:1
4:1
D
MCF-7
SKBR-3
% max
HER-2
isotype
Mean Fluorescence Intensity

Suppl Fig.6

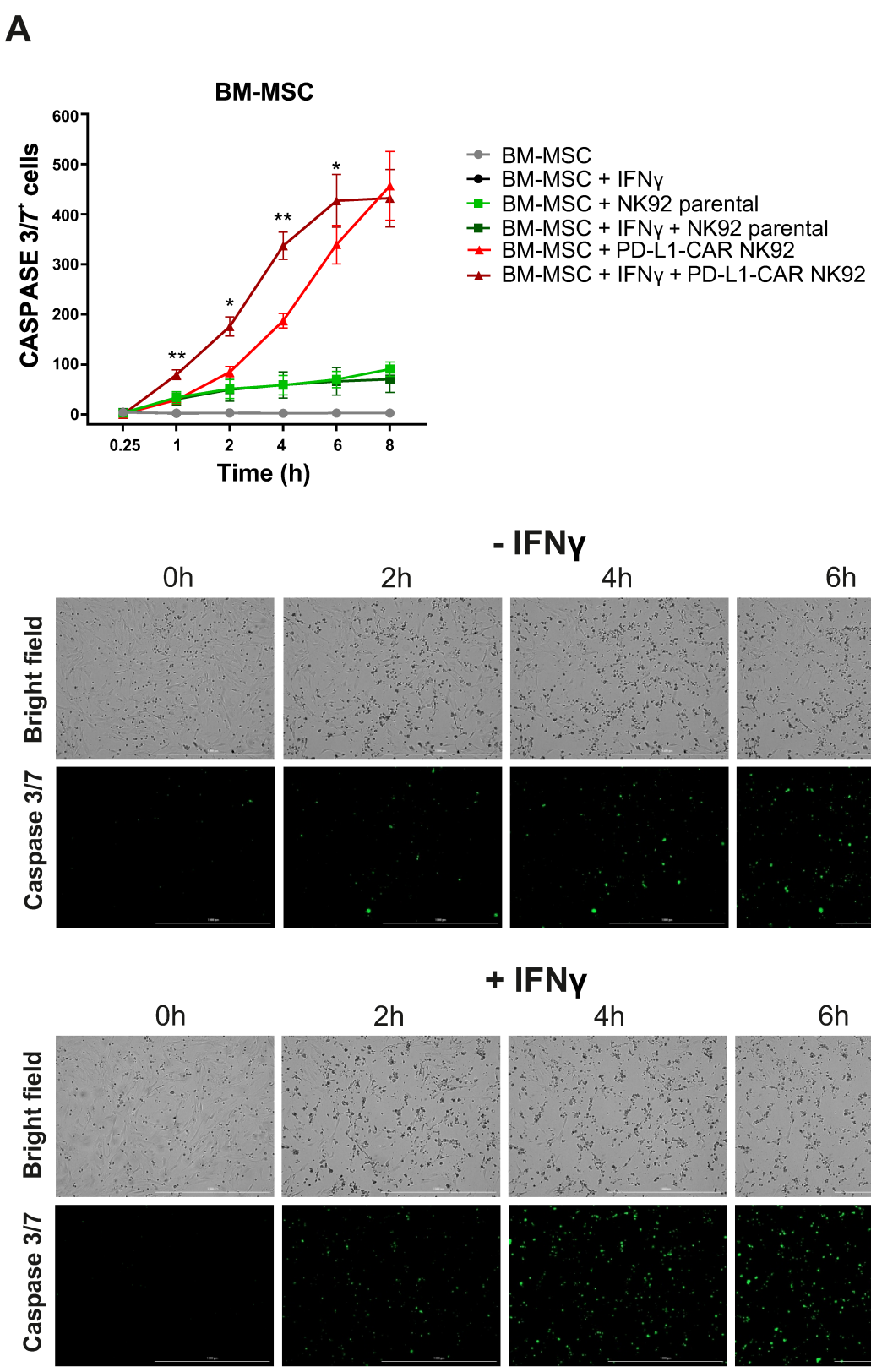
A
BM-MSC
CASPASE 3/7+ cells
Time (h)
BM-MSC
BM-MSC + IFNγ
BM-MSC + NK92 parental
BM-MSC + IFNγ + NK92 parental
BM-MSC + PD-L1-CAR NK92
BM-MSC + IFNγ + PD-L1-CAR NK92
- IFNγ
+ IFNγ
0h
2h
4h
6h
8h
Bright field
Caspase 3/7

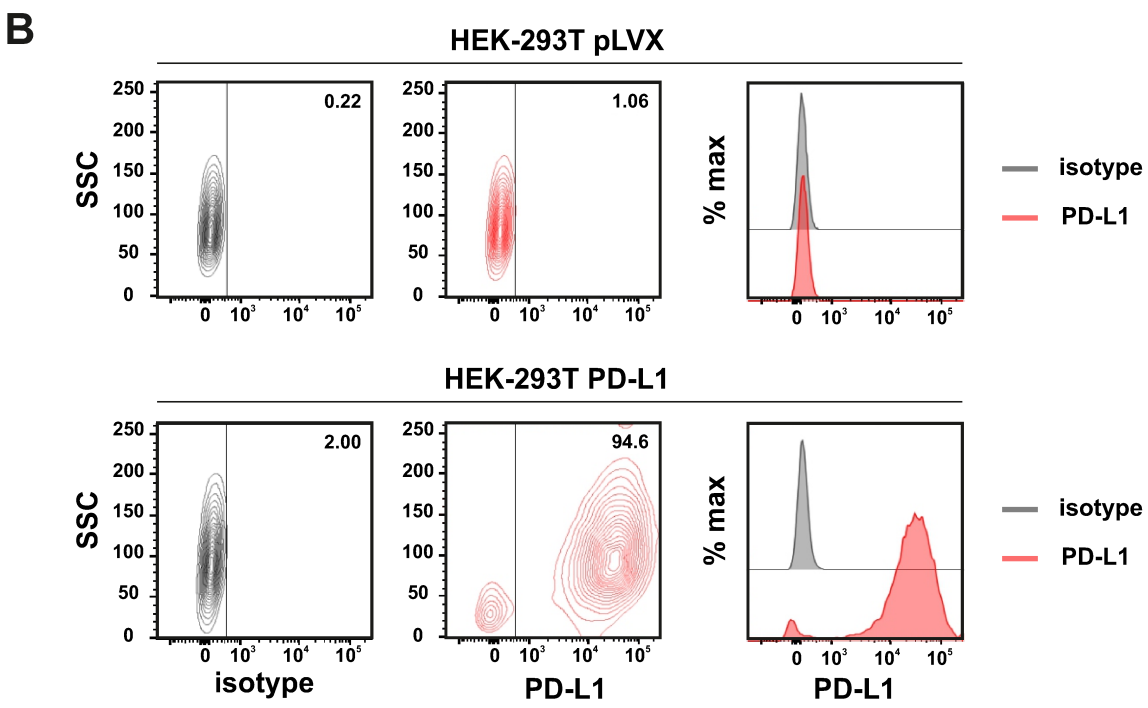
B
HEK-293T pLVX
HEK-293T PD-L1
SSC
% max
isotype
PD-L1
0.22
1.06
2.00
94.6

Suppl Fig. 7